

2017-01-30

# Combined sea-level and climate controls on limestone formation, hiatuses and ammonite preservation in the Blue Lias Formation, South Britain (uppermost Triassic Lower Jurassic)

WEEDON, GRAHAMP

<http://hdl.handle.net/10026.1/8505>

---

10.1017/S001675681600128X

Geological Magazine

Cambridge University Press (CUP)

---

*All content in PEARL is protected by copyright law. Author manuscripts are made available in accordance with publisher policies. Please cite only the published version using the details provided on the item record or document. In the absence of an open licence (e.g. Creative Commons), permissions for further reuse of content should be sought from the publisher or author.*

1  
2  
3  
4  
5  
6  
7  
8  
9  
10  
11  
12  
13  
14  
15  
16  
17  
18  
19  
20  
21  
22  
23  
24

**Combined sea-level and climate controls on limestone formation, hiatuses and ammonite preservation in the Blue Lias Formation, South Britain (uppermost Triassic–Lower Jurassic)**

Short title/running head: **Sea level and climate controls of the Blue Lias**

Graham P. Weedon<sup>1\*</sup>, Hugh C. Jenkyns<sup>2</sup> and Kevin N. Page<sup>3</sup>

\* Corresponding author

**1** [graham.weedon@metoffice.gov.uk](mailto:graham.weedon@metoffice.gov.uk), Met Office, Maclean Building, Benson Lane, Crowmarsh Gifford, Wallingford, Oxfordshire, OX10 8BB, UK.

**2** Department of Earth Sciences, University of Oxford, South Parks Road, Oxford, OX1 3AN, UK.

**3** School of Geography, Earth and Environmental Sciences, Plymouth University, Drake Circus, Plymouth, PL4 8AA, UK.

In press: *Geological Magazine*

January 2017

25           **Abstract**

26           Lithostratigraphic and magnetic-susceptibility logs for four sections in the Blue Lias  
27 Formation are combined with a re-assessment of the ammonite biostratigraphy. A Shaw plot  
28 correlating the West Somerset coast with the Devon/Dorset coast at Lyme Regis, based on 63  
29 common biohorizon picks, together with field evidence, demonstrate that intra-formational  
30 hiatuses are common. Compared to laminated shale deposition, the climate associated with  
31 light marl is interpreted as both drier and stormier. Storm-related non-deposition favoured  
32 initiation of limestone formation near the sediment-water interface. Areas and time intervals  
33 with reduced water depths had lower net accumulation rates and developed a greater proportion  
34 of limestone.

35           Many homogeneous limestone beds have no ammonites preserved, whereas others  
36 contain abundant fossils. Non-deposition encouraged shallow sub-seafloor cementation which,  
37 if occurring after aragonite dissolution, generated limestones lacking ammonites. Abundant  
38 ammonite preservation in limestones required both rapid burial by light marl during storms as  
39 well as later storm-related non-deposition and near-surface carbonate cementation that  
40 occurred prior to aragonite dissolution.

41           The limestones are dominated by a mixture of early framework-supporting cement that  
42 minimized compaction of fossils, plus a later micrograde cement infill. At Lyme Regis, the  
43 relatively low net accumulation rate ensured that final cementation of the limestones took place  
44 at relatively shallow burial depths. On the West Somerset coast, however, much higher  
45 accumulation rates led to deeper burial before final limestone cementation. Consequently, the  
46 oxygen-isotope ratios of the limestones on the West Somerset coast, recording precipitation of  
47 the later diagenetic calcite at higher temperatures, are lower than those at Lyme Regis.

48

49   **Keywords:**

50 Sedimentary cycles; Sea level; Climatic cycles; Blue Lias Formation; Diagenesis; Hiatuses

51

## 52 **1. Introduction**

53 The origin and significance of the limestone beds and nodules in the uppermost  
54 Rhaetian (Triassic) to Sinemurian (Jurassic) Blue Lias Formation of Britain has long been a  
55 subject of interest (Day, 1865; Richardson, 1923; Kent, 1936). Hallam (1960; 1964) argued  
56 that the limestones owed their characteristics to both diagenetic and primary (i.e. depositional)  
57 factors. Shukri (1942) speculated on the possible role of climate but ruled out forcing by  
58 Milankovitch orbital-precession cycles because the limestone beds at Lyme Regis are more  
59 widely spaced in the lower Sinemurian compared to the Hettangian. Following the  
60 demonstration by Hays, Imbrie & Shackleton (1976) of orbital forcing of Pleistocene to Recent  
61 climate, House (1985; 1986) and Weedon (1985; 1986) revived the idea of orbital-climatic  
62 (Milankovitch cycle) forcing to explain the interbedded lithologies.

63 One of the reasons the Blue Lias Formation has attracted so much research interest is  
64 that it exhibits two styles of sedimentary cyclicity. Visually most obvious are the alternations  
65 of limestones and non-limestones, but also present are alternations of homogeneous, organic-  
66 carbon-poor strata (grey limestone plus light grey marl) with laminated organic-carbon-rich  
67 strata (black to very dark grey laminated shale plus laminated limestone). Dark grey marls  
68 represent intermediate compositions. The homogeneous limestone beds and layers of nodules  
69 are considered to have formed diagenetically within light marl beds while the much rarer  
70 laminated limestone beds and laminated limestone nodules formed within primary laminated  
71 shale beds (Hallam, 1964; Weedon, 1986; 1987a; Arzani, 2004).

72 Weedon (1986; 1987a) showed, using time-series analysis, that the alternation of the  
73 limestone with the non-limestones can encode a similar signal of regular cycles to that of the  
74 alternating homogeneous and laminated rock types. However, in thicker sections such as those

75 exposed on the West Somerset Coast, multiple limestone beds and/or nodule horizons occur  
76 within thick (tens of centimetre- to metre-scale) light marl beds. A recent analysis of orbital  
77 forcing in the relatively thick sections on the West Somerset Coast (Ruhl *et al.*, 2010)  
78 specifically avoided sampling the limestones that nonetheless represent a critical part of the  
79 sequence. This paper is designed to clarify the nature of the information conveyed by the  
80 limestones, both laminated and homogeneous.

81 ----- Figure 1 near this position -----

82 New, high-resolution lithostratigraphic and magnetic-susceptibility logs for four  
83 sections (Fig. 1) are presented together with refinements of the ammonite biostratigraphy. The  
84 sections chosen within ‘typical offshore’ Blue Lias, span all the ammonite zones of the  
85 Hettangian Stage and represent a wide range of net accumulation rates. The aims are to explain  
86 why: a) limestone bed thicknesses are apparently independent of the net accumulation rate; b)  
87 the spacing of the limestone beds within ammonite zones can be related to Milankovitch orbital  
88 cycles although there are large variations in spacing from zone to zone and from place to place;  
89 c) laminated limestone beds and laminated limestone nodules are comparatively rare; and d)  
90 some limestone beds preserve abundant ammonite fossils, but others preserve none. We present  
91 new evidence for intra-formational hiatuses and a synthesis of limestone formation in terms of  
92 combined climatic and sea-level controls plus an improved understanding of the preservation  
93 of the ammonites.

94

## 95 **2. Bio- and chronostratigraphy**

### 96 **2.a. Ammonite biochronology and correlation**

97 The Jurassic System is divided into a sequence of 11 globally applicable stages that are  
98 subdivided, without gaps or overlap, into regional sequences of ammonite-correlated ‘zones’  
99 (Ogg & Hinnov, 2012). Since ammonite zones completely fill each stage, and are now usually

100 explicitly defined with a basal stratotype, they can also be considered to be  
101 chronostratigraphical units (Callomon, 1985; 1995; Page, 1995; 2003; in press). The great  
102 majority of zones do not conform in any way to a classical biozone since they do not correspond  
103 to the range of any ammonite species or assemblage.

104         In the present work, we refer neutrally to the ammonite-correlated stratigraphical units  
105 as ‘Standard’ Zones and Subzones (*sensu* Callomon, 1985), rather than using an epithet to  
106 describe their character (i.e. ‘chronozone’ and ‘subchronozone’ as in Page, 2010a; 2010b;  
107 2010c). However, as chronozones, these units can be explicitly correlated using proxies other  
108 than ammonites, such as local lithological changes, other faunal or floral elements and isotopic  
109 ‘events’ (Jenkyns *et al.*, 2002).

110         Throughout the Jurassic System, infra-subzonal units that are often referred to as  
111 biohorizons provide a very high-resolution biochronology. Biohorizons typically correspond  
112 to the stratigraphic range of a specific indicator species. Normally, the bases of ammonite  
113 Standard Zones are explicitly, or effectively, defined by the bases of specific biohorizons, and  
114 hence correlated, as potential timelines, by the stratigraphically lowest occurrences of the  
115 indicator species.

116         The initial biohorizontal framework for the Lower Sinemurian Stage in the UK of Page  
117 (1992) led to the schemes applied by Page (2002; 2010b) to the Devon and Dorset coastal  
118 sections. The scheme for the Hettangian Stage of the Devon/Dorset coast (Page, 2010b; 2010c)  
119 was based largely on the version for West Somerset by Page (2005), but recent re-sampling of  
120 the latter area has revealed even greater biostratigraphical detail, which is used here. This new  
121 scheme provides a sequence of 55 biohorizons for the Hettangian, as opposed to the 27 used  
122 by Page (2010b; 2010c).

123         Zonal and subzonal boundaries throughout the Hettangian have been reviewed, based  
124 on new sampling by K.N.P. on coastal sections (Fig. 1a) in East Devon (Lyme Regis), West

125 Somerset (Doniford, St Audries Bay, East Quantocks Head to Kilve) and South Glamorgan,  
126 South Wales (St. Mary's Well Bay, Lavernock). The biohorizon boundaries, where constrained  
127 to within a few centimetres stratigraphically, are indicated in Table 1. Within the Lower  
128 Sinemurian of West Somerset, the placement of biohorizon boundaries are as previously  
129 published (e.g. Bloos & Page, 2000b; Page 2010b; 2010c).

130

131 -----Table 1 near this position-----

132

### 133 **2.b. The base of the Jurassic**

134 The Global Stratigraphic Section and Point (GSSP) for the base of the Jurassic has been  
135 defined in the Kuhjoch section in the Austrian Calcareous Alps (Hillebrandt, Krystyn &  
136 Kuerschner, 2007; Hillebrandt & Krystyn, 2009). Subsequently Page (2010b; 2010c) revised  
137 the zonal framework for the base of the Hettangian Stage in the UK by inserting the former  
138 authors' Tilmanni Zone below the Planorbis Zone (which was previously considered to be the  
139 lowest zone of the Jurassic System).

140 Page (2010b; 2010c) concluded that only the top of the Tilmanni Zone in the UK had  
141 yielded ammonites, specifically *Psiloceras erugatum* (Phillips) as illustrated by Bloos & Page  
142 (2000a). Nevertheless, in the UK the base of the Zone and hence the base of the Jurassic System  
143 can still be approximated using the most positive part of a positive  $\delta^{13}\text{C}_{\text{org}}$  interval, as  
144 demonstrated by Clémence *et al.* (2010). At St Audries Bay on the West Somerset coast (Fig.  
145 1), the base of the Hettangian corresponds to a level less than 1.5 m above the base of the Blue  
146 Lias Formation (Clémence *et al.*, 2010). At St Mary's Well Bay near Lavernock, South Wales  
147 (Fig. 1), the  $\delta^{13}\text{C}_{\text{carb}}$  curve of Korte *et al.* (2009), based on measurements of *Liostrea* sp.  
148 samples, suggests that the base of the Jurassic System lies about 1.9 m above the top of the  
149 Langport Member (Penarth Group, Upper Triassic). The  $\delta^{13}\text{C}_{\text{carb}}$  curve produced from bulk

150 sediment samples from the coast at Lyme Regis on the Devon/Dorset border by Korte *et al.*  
151 (2009) is, however, of limited use for correlation because it does not show the same signature  
152 as elsewhere. Nevertheless, it is likely that the base of the Jurassic System in the area also lies  
153 in the lowest part of the Blue Lias Formation.

154

### 155 **2.c. The base of the Planorbis Zone**

156 The base of the Planorbis Zone, as correlated by the first appearance of *Neophyllites* at  
157 the base of the Hn3 *imitans* Biohorizon (Page, 2010a), corresponds to the base of bed 9 of  
158 Whittaker & Green (1983) on the West Somerset Coast (Page & Bloos, 1995; Bloos & Page  
159 2000a). In South Glamorgan, in St. Mary's Well Bay, Lavernock, the base of the Planorbis  
160 Zone is about 12 cm below the base of bed 30 of Waters and Lawrence (1987): i.e. the level  
161 indicated by Hodges (1994) within his bed 38. At Lyme Regis, this level correlates with the  
162 base of bed H25 of Lang (1924); see Page (2002).

163

### 164 **2.d. Southam Quarry near Long Itchington**

165 At Southam Quarry, Long Itchington, Warwickshire, below bed 10 of Clements *et al.*  
166 (1975; 1977) ammonites are rare (Radley, 2008) and the lowest part of the Blue Lias Formation  
167 is inferred to belong to the Liasicus Zone (i.e. the Tilmanni and Planorbis zones are missing).  
168 This interpretation follows from the location of Long Itchington in relation to the reconstructed  
169 age of onlap of the Blue Lias Formation onto the London-Brabant Platform by Donovan,  
170 Horton & Ivimey-Cook (1979). Furthermore, it is consistent with the records of Old, Sumbler,  
171 & Ambrose (1984, p. 34), who cite *Laqueoceras* and *Waehneroceras* 'close above the Langport  
172 Member' at Southam Quarry. *Laqueoceras* certainly indicates the lower part of the Laqueus  
173 Subzone Hn18 Biohorizon of Page (2010b; 2010c). However, specimens of *Waehneroceras*  
174 from Southam Quarry include species from the upper part of the Portlocki Subzone, including



175 abundant examples of *W. portlocki* (Wright), in limestone nodules and rare *W. cf. shroederi*  
176 Lange in limestone beds. These observations suggest that at least biohorizons Hn16 and Hn17  
177 of Page (2010b; 2010c) are also present.

178

### 179 **3. The sections studied and the lithostratigraphic and magnetic-susceptibility logs**

180 Lithological logging, whilst measuring magnetic susceptibility (MS) in the field,  
181 utilized the five microfacies or rock-types of Weedon (1986; 1987a), as adopted by others (e.g.  
182 Bottrell & Raiswell 1989, Arzani 2004; 2006; Paul, Allison & Brett 2008) i.e. homogeneous  
183 grey limestone, laminated grey limestone, light grey marl, dark grey marl and millimetre-  
184 laminated black shale. Limestone nodules occur within light marl beds and locally pass  
185 laterally into continuous limestone beds (e.g. at Lyme Regis bed 37 or ‘Rattle’: Lang (1924)  
186 and Hesselbo & Jenkyns (1995) provide all the limestone bed names for the Devon/Dorset  
187 coast). Laminated limestone nodules occur within the laminated black shales. Large differences  
188 in net accumulation rates in the sections studied are suggested by the thicknesses of zones  
189 shown in Fig. 1b, and the average composition of the rock-types is indicated in Fig.1c and  
190 discussed further in Section 4.

191

#### 192 **3.a. Measurements of magnetic susceptibility in the field**

193 Volume magnetic susceptibility (vol MS) logging of sections used a Bartington  
194 Instruments MS2 meter combined with an F-probe in direct contact with fresh faces of rock at  
195 right angles to the bedding. Instrument drift, related to temperature changes, was removed by  
196 taking measurements in the air more than 1 metre from the cliff face between each rock-surface  
197 measurement. At the levels of limestone nodules, MS was measured in the limestone rather  
198 than light marl in cases where limestone constituted more than half of that stratigraphic level  
199 (Weedon *et al.*, 1999). As far as possible, calcite ‘beef’ veins and lenses (Richardson, 1923;

200 Marshall, 1982), most prevalent at the base of laminated shale beds at Lyme Regis, were  
201 avoided during MS measurement.

202 ----- Figure 2 near this position -----

203 Measurements of weight-specific MS (wt MS) using a Bartington Instruments MS2B  
204 sensor for samples from Lyme Regis, and the West Somerset coast show the expected strong,  
205 linear correlation with vol MS (Pearson's  $r = +0.967$ ,  $N = 74$ ,  $P < 0.001$ , Fig. 2a). This  
206 relationship and the similarity of both the vol MS and wt MS logs to %CaCO<sub>3</sub> in Fig. 2b  
207 confirm that the field measurements are neither significantly affected by changes in magnetic  
208 properties due to weathering, nor by incomplete rock sensing due to imperfect surface contact  
209 and/or undetected voids.

210 The lithological columns shown in Figs 3–6, with captions indicating the references  
211 used in bed numbering, illustrate large variations in the thickness of the marls and shales and  
212 highly variable spacing and overall proportions of limestone beds. In the logs, the laminated  
213 black shales are shown as the most recessed lithology on the profiles as a convention to aid  
214 their identification rather than as an indication of the lowest resistance to weathering. The fixed  
215 spacing of the MS measurements at each section was designed to resolve the smallest variations  
216 in bulk composition. The measurements were obtained at 2 cm spacing at Lyme Regis; 3 cm  
217 at Southam Quarry, Long Itchington and 4 cm spacing on both the West Somerset coast and at  
218 St. Mary's Well Bay, Lavernock. In Southam Quarry, the faces were measured for magnetic  
219 susceptibility in 1994 when the section in the south west between the A423 and the A426 was  
220 fully accessible down to the disconformity with the Upper Triassic Langport Member. The vol  
221 MS log for Lyme Regis was reported previously (Weedon *et al.*, 1999) but Fig. 4, primarily of  
222 the Hettangian portion, shows revisions to the zonal and subzonal boundaries.

223 ----- Figure 3 near this position -----

224 The log for the West Somerset coast (Fig. 5a and b; Palmer, 1972; Whittaker & Green,  
225 1983) is composite. The section at St Audries Bay was measured from the base of the Blue  
226 Lias Formation to the top of bed 101 of Whittaker & Green (1983), overlapping the MS log at  
227 Quantock's Head by about 3.5 m. The Quantock's Head to Kilve section was measured for MS  
228 from bed 97 to bed 163. The splice level of the composite record in bed 96, at 56.90 m above  
229 the base of the Blue Lias Formation, represents the base of the Quantock's Head magnetic-  
230 susceptibility log. Note that in Table 1 the biohorizon levels of the Quantock's Head section  
231 are listed both relative to the base of the log (i.e. at the splice level) and relative to the base of  
232 the Formation according to the heights of the St Audries Bay section within the composite  
233 column.

234 ----- Figure 4 near this position -----

235

### 236 **3.b. Origin of the variations in vol MS**

237 It was reported previously for the Blue Lias Formation that MS is inversely correlated  
238 with %CaCO<sub>3</sub> (Hounslow, 1985; Weedon *et al.*, 1999; Deconinck *et al.*, 2003; Ruhl *et al.*,  
239 2010). This relationship is supported by current measurements of wt MS using a Bartington  
240 Instruments MS2B cavity sensor and vol MS (Fig. 2a). The right-hand linear regression line of  
241 Fig. 2a allows estimation of carbonate contents from the field measurement of vol MS (using:  
242 %CaCO<sub>3</sub> = 99.06 – (13.79 x vol MS),  $r = -0.892$ ,  $N = 74$ ,  $P < 0.001$ ). Calcium carbonate  
243 measurements have been shown as open circles on top of the MS logs in Figs 4 and 5 by scaling  
244 %CaCO<sub>3</sub> (bottom scale) relative to the vol MS (top scale) according to this regression. Despite  
245 the good agreement between the estimated and measured %CaCO<sub>3</sub> shown on the right of Fig  
246 2b, the uncertainty (95% confidence interval) in individual estimates of %CaCO<sub>3</sub> from vol MS  
247 using the regression is about ±20.0% – ranging between ±19.6 and ±20.4%, depending on the  
248 difference between the individual vol MS and the mean vol MS (Williams, 1984, p. 313).

249 ----- Figure 5a near this position -----

250 ----- Figure 5b near this position -----

251 The average MS values for these mudrocks are fairly low, thereby contrasting with  
252 younger British Jurassic cyclic mudrocks such as the Kimmeridge Clay Formation (Weedon *et*  
253 *al.*, 1999). It was shown for the Blue Lias Formation (Hounslow, 1985; Bixler, Elmore &  
254 Engel, 1998; Deconinck *et al.*, 2003; Hounslow, Posen & Warrington, 2004) that the  
255 stratigraphic variations in MS are consistent with variable dilution of paramagnetic clays by  
256 non-ferroan, and thus diamagnetic, calcite (wt MS =  $+0.84 \times 10^{-8}$  SI, Bleil & Petersen, 1987).  
257 Note that despite the presence of locally rather large percentages of pyrite (maximum 12% in  
258 the laminated shales, Weedon, 1987a) in a pure, unweathered, state this mineral is also  
259 diamagnetic (wt MS =  $-0.48 \times 10^{-8}$  SI, Collinson, 1983) and consequently contributes very little  
260 to the whole-rock MS signal. Hence, stratigraphic logs of MS in the Blue Lias Formation  
261 provide an accurate picture of the occurrence of the limestones (Figs 2a, 2b and 3).

262 The marls and shales of the Liasicus Zone at all four localities have consistently higher  
263 average MS than the underlying Tilmanni and Planorbis and overlying Angulata and Bucklandi  
264 zones (Figs 3–6, Weedon *et al.*, 1999; Deconinck *et al.*, 2003). This observation suggests that  
265 there were long-term (zonal-scale) variations in the composition of the paramagnetic (mainly  
266 clay mineral) components (Deconinck *et al.*, 2003). The relatively high average MS of the  
267 lower part of the section in Southam Quarry (Fig. 6) is consistent with the interpretation  
268 (Section 2.d) that the lowermost strata that lie disconformably on the Langport Member belong  
269 to the Liasicus Zone and not to the Planorbis Zone.

270 At about the 31 m level in the mid-Liasicus Zone (upper Portlocki Subzone) of the St  
271 Audries Bay section (Fig. 5a), the average vol MS is unusually high with values extending  
272 outside the range of the %CaCO<sub>3</sub> versus vol MS regression of Fig. 2a. Lower stratigraphic  
273 resolution sampling by Deconinck *et al.* (2003) indicates that, at this level on the West

274 Somerset coast, the clay minerals switch to higher kaolinite/illite ratios, but surprisingly, not  
275 to iron-rich clays. The unusually high MS might indicate an association of increased kaolinite  
276 with a source of different paramagnetic components and/or small amounts of ferromagnetic  
277 components such as magnetite-like minerals that, unusually for the Blue Lias Formation,  
278 survived dissolution by H<sub>2</sub>S during diagenesis (Deconinck *et al.*, 2003). A similar interval of  
279 unusually high values of vol MS, of around 8.0 x10<sup>-8</sup> SI, is found at about 8.2 m in Southam  
280 Quarry in the Liasicus Zone (Fig. 6). This interval of high average MS in the marls and shales  
281 is located at the top of the Portlocki subzone, Liasicus Zone at both St Audries and Lyme Regis  
282 and may provide a correlatable change in paramagnetic mineralogy (Figs 4 and 5a).

283 ----- Figure 6 near this position -----

284

#### 285 **4. Variations in whole-rock composition**

286 The typical ‘offshore’ facies of the Hettangian Blue Lias Formation of interest here  
287 shows considerable lateral and stratigraphic variations in bulk composition as discussed in  
288 Sections 4.b and 4.c. To provide a context for these descriptions we start with consideration of  
289 the ‘marginal facies’.

290

##### 291 **4.a. Marginal facies and ‘near-shore’ Blue Lias**

292 The Blue Lias was deposited at the same times as palaeo-coastline deposits that include  
293 the Sutton Stone and Southerndown Beds of South Glamorgan (Trueman, 1920; 1922; Hallam,  
294 1960; Wobber, 1965; Fletcher, 1988; Sheppard, 2006) and the Brockley Down Stone of the  
295 Radstock Plateau near Bristol (D. L. Loughman, unpub. Ph.D. thesis, University of  
296 Birmingham, 1982; Donovan & Kellaway, 1984). These so-called marginal facies, formed at  
297 and close to palaeo-coastlines, lie unconformably on Carboniferous Limestone and comprise

298 conglomeratic limestones with grainstone textures including Carboniferous Limestone and  
299 chert lithoclasts, derived bioclasts, ooids and bioclasts (Wobber, 1965; 1966; Fletcher, 1988).

300         On the coast near Southerndown, Glamorgan, 31 km west north west of the exposure  
301 at Lavernock (Fig. 1a), the unconformity surface is exposed and consists of multiple wave-cut  
302 platforms overlain by associated successive breccia and conglomeratic and grainstone  
303 limestones of the Sutton Stone (Fletcher, 1988; Sheppard, 2006). Both the unconformity  
304 surface and Carboniferous Limestone lithoclasts in the overlying Sutton Stone have *Trypanites*  
305 borings and are encrusted by oysters and colonial corals (Johnson & McKerrow, 1995; Simms,  
306 Little & Rosen, 2002; Sheppard, 2006). Some lithoclasts in the Sutton Stone are imbricated  
307 (Wobber, 1963) and elongate bioclasts have been used as palaeocurrent indicators that indicate  
308 long-shore drift and complex current movements influenced by the local islands of  
309 Carboniferous rocks (Wobber, 1966). The matrix-supported and rounded boulder- and cobble-  
310 sized lithoclasts in the Sutton Stone are succeeded stratigraphically by pebble-grade lithoclasts,  
311 micrites and thin shales of the Southerndown Beds, which grade laterally into the near-shore  
312 facies of Blue Lias (Trueman, 1922; Wobber, 1965; Wilson et al., 1990; Sheppard, 2006).

313         Although the platform erosion probably started in the latest Triassic, ammonites have  
314 been recovered in stratigraphic order from the Sutton Stone and Southerndown Beds from the  
315 Planorbis, Liasicus and Angulata Zones (Hodges, 1986; Sheppard, 2006). These observations  
316 are not consistent with nearly instantaneous deposition of the Sutton Stone by a single hurricane  
317 (Ager, 1986), but rather with the latest Triassic and Early Jurassic erosion of the wave-cut  
318 platforms and deposition of the marginal facies under storm influence over millions of years  
319 during episodic rises in relative sea level (Trueman, 1922; Fletcher, 1988; Sheppard, 2006).

320         Just six kilometres south of the palaeo-coastline of Southerndown at Nash Point, the  
321 Blue Lias of the Bucklandi Zone represents an atypical limestone-dominated facies often full  
322 of bioclast fragments in both the marls and limestones (Hallam, 1960; Weedon, 1987a;

323 Trueman, 1930). These strata representing Units B and C of the Porthkerry Formation have  
324 much higher limestone proportions than found in more 'typical' Blue Lias (an average of 60 to  
325 85 % limestone by thickness in sections tens of metres thick, Waters & Lawrence, 1987; Wilson  
326 et al., 1990; Warrington & Ivimey-Cook, 1995). Units B and C consist of metre-scale bedding  
327 units formed of closely spaced nodular limestones and 'anastomosing mudstone beds' that  
328 probably result from pressure dissolution (Waters & Lawrence, 1987). Local decimetre-scale  
329 mudstone beds are present, permitting correlation of limestone-shale bed groups, but organic-  
330 carbon contents are low and neither laminated shales nor laminated limestones are present  
331 (Sheppard, Houghton & Swan, 2006). Although much of the bedding was formed purely during  
332 diagenesis, the presence of hummocky cross-stratification at Nash Point proves strong storm  
333 influences (Sheppard, Houghton & Swan, 2006).

334         Thirty kilometres from the palaeo-coastline of South Glamorgan, typical 'offshore'  
335 Blue Lias facies is present at Lavernock in the Tilmanni to Liasicus zones as logged here (Fig.  
336 3). In the lower part of the Angulata Zone Unit A of the Porthkerry Formation consists of about  
337 55 % by thickness of normal offshore Blue Lias with nodular limestones and marls. However,  
338 in the same area near Cardiff, the upper part of the Angulata Zone, 'Unit B' of the Porthkerry  
339 Formation of Waters and Lawrence (1987), is of a similar facies to the Bucklandi Zone at Nash  
340 Point. The Porthkerry Formation is overlain gradationally by uppermost Angulata Zone and  
341 Bucklandi Zone oolitic 'marginal facies' (Waters & Lawrence, 1987). Thus, Units B and C of  
342 the Porthkerry Formation near Cardiff and Nash Point represent a 'near-shore' facies of the  
343 Blue Lias, which has been envisaged as a storm-derived aragonitic lime mud deposited on a  
344 marine shelf (Sheppard, Houghton & Swan, 2006).

345

#### 346                   **4.b. Rock-type compositions**

347           The different rock-types of the ‘typical’ or ‘offshore’ Blue Lias consist mostly of  
348 various proportions of bioclasts, calcite microspar, clay minerals, organic matter, pyrite and  
349 minor quartz silt (Hallam, 1960; Weedon, 1986; 1987a). Whole rock compositions quoted here  
350 are based on the samples from both Lyme Regis and the Somerset Coast (Weedon, 1987a).  
351 Numbers of samples by rock type and locality are indicated in the caption for Fig. 1c and  
352 sample locations are indicated in Figs 4 and 5. The limestones (total organic carbon, TOC,  
353 mean = 0.54% ± 0.09 (±95% confidence interval), range = 0.14 to 1.64%,  $N = 48$ ; CaCO<sub>3</sub>,  
354 mean = 79.3% ± 2.2, range = 51.8 to 88.7%,  $N = 48$ ) form beds with contacts ranging from  
355 planar to nodular. Limestone nodules are typically entirely enclosed by light marl but can be  
356 ‘welded’ onto limestone beds. On the Devon/Dorset and West Somerset coasts, when seen in  
357 plan on the foreshore, limestone nodules are often found to be linked laterally at some levels.  
358 The limestones generally have a homogeneous bioclastic wackestone to bioclastic carbonate  
359 mudstone fabric reflecting the thoroughly bioturbated nature of the precursor light marls. The  
360 light marls (TOC mean = 1.42% ± 0.26, range = 0.38 to 4.41%,  $N = 40$ ; CaCO<sub>3</sub>, mean = 43.8%  
361 ± 2.7, range = 25.7 to 69.9%,  $N = 40$ ) are friable and homogeneous with planar contacts against  
362 dark marls and laminated shale beds.

363           Normally the dark marls (TOC mean = 2.35% ± 0.41, range = 0.51 to 6.51%,  $N = 39$ ;  
364 CaCO<sub>3</sub>, mean = 40.1% ± 3.7, range = 19.9 to 61.0%,  $N = 39$ ) are homogeneous like the light  
365 marls and friable, but can become fissile on weathering. However, Fig. 7a shows a laminated  
366 dark marl fabric, not visible in the field, consisting of abundant microspar lenses in places  
367 forming nearly continuous laminae that alternate with other laminae comprising clay and  
368 organic matter (Weedon, 1987a). The figure shows a *Chondrites* burrow with a homogeneous  
369 light marl filling that penetrates the dark marl fabric. Burrow mottles at the contacts of light  
370 and dark marl beds are common at Lyme Regis as both light marl burrow-fills within dark marl  
371 and *vice versa* (Hallam, 1964).



372 The laminated shales (TOC mean = 5.46% ± 0.77, range = 1.53 to 12.80%,  $N = 51$ ;  
373  $\text{CaCO}_3$ , mean = 35.5% ± 3.4, range = 11.6 to 68.4%,  $N = 51$ ), usually with sharp basal bedding  
374 contacts against dark marl or light marl, produce a brown streak when scratched and weather  
375 into fissile, sometimes paper thin, laminae. Sub-microscopically they have scattered calcite  
376 microspar lenses dispersed within wavy sub-millimetre laminae of clay and organic matter  
377 (Weedon, 1987a). Laminated limestone (TOC mean = 1.42% ± 0.67, range = 0.90 to 3.00%,  $N$   
378 = 7;  $\text{CaCO}_3$ , mean = 77.2% ± 6.2, range = 62.4 to 87.2%,  $N = 9$ ) forms beds that have planar  
379 contacts with laminated shale beds or nodules that are enclosed entirely by laminated shale  
380 (Weedon, 1987a; Arzani, 2004).

381 ----- Figure 7 near this position -----

382 Hallam (1987) and Arzani (2006) doubted the presence of rock-forming quantities of  
383 nannofossils as a possible precursor to the microspar. However, calcareous nannofossils, both  
384 as true coccoliths as well as *Schizosphaerella*, are well documented from throughout the  
385 Tilmanni to Bucklandi zone interval at Lyme Regis and on the West Somerset coast (Hamilton,  
386 1982; Bown, 1987; Bown & Cooper, 1998; Van de Schootbrugge *et al.*, 2007; Clémence *et al.*,  
387 2010). Indeed, Weedon (1986; 1987a; 1987b) argued that the microspar lenses in the dark marls  
388 and laminated shales represent neomorphosed zooplankton faecal pellets containing calcareous  
389 nannofossils. Very similar fabrics to Fig. 7a are known in the Kimmeridge Clay Formation of  
390 Dorset (Kimmeridgian to Tithonian, Fig. 2d, f and g of Pearson, Marshall & Kemp, 2004),  
391 which has abundant nannofossils (e.g. Young & Bown, 1991; Lees, Bown & Young, 2006).  
392 Aggregates of nannofossils surrounded by clay minerals and organic matter in the Blue Lias  
393 Formation (Figs 8b, 8c and 8d; figure 3 of Weedon, 1986; figures 6B and 6C of Arzani, 2006)  
394 have similar dimensions to the microspar lenses, supporting their interpretation as  
395 neomorphosed zooplankton faecal pellets (Pearson, Marshall & Kemp, 2004).

396 Weedon (1986; 1987a) argued that nannofossil preservation was best in the more  
397 organic carbon-rich laminated shales and dark marls, as confirmed recently by Clémence *et al.*  
398 (2010). The high organic-carbon contents may have helped the preservation of primary organic  
399 coatings on the coccoliths, which in turn prevented calcite dissolution by acidic pore waters  
400 during diagenesis (Bukri, Dent Glasser & Smith, 1982). In the less organic-carbon-rich  
401 sediments, partial or total microspar aggradation of nannofossils (e.g. Fig. 8b) was inferred to  
402 be the normal situation in the Blue Lias (Weedon, 1986; 1987a; 1987b). The homogeneity of  
403 the light marls and most of the dark marls was explained as resulting from burrowers mixing  
404 the organic-matter- and clay-rich laminae with faecal pellets. In the limestones and light marls,  
405 however, very rare isolated elliptical structures, representing partially corroded or overgrown  
406 coccoliths provide the only *in situ* evidence for calcareous nannofossil precursors to the  
407 microspar (Fig. 8e; Fig. 2.4B of Weedon, 1987a).

408 If most carbonate mud in the ‘offshore’ Blue Lias Formation was derived from very  
409 shallow coastal waters rather than from nannofossil material, different localities would be  
410 expected to have different rock-type compositions. However, the average %CaCO<sub>3</sub> and %TOC  
411 of the limestone, light marl, dark marl and laminated shales are statistically indistinguishable  
412 between the Devon/Dorset coast and the West Somerset coast sections (i.e. overlapping 95%  
413 confidence intervals in Fig. 1c). Therefore, considering the large difference in zonal and  
414 average bed thicknesses between these locations, the lithological composition of the offshore  
415 Blue Lias facies was not influenced by either the local net accumulation rates or by local  
416 differences in water depth. The consistency of facies between localities and across the range of  
417 accumulation rates represented is consistent with a primarily hemipelagic, rather than  
418 shoreline-influenced origin for the carbonate mud (Weedon, 1986).

419 The majority of the laminated limestone beds were formed by the coalescence of  
420 laminated limestone nodules (Weedon, 1987a; Arzani, 2004). However, at Lyme Regis, bed

421 H30 categorized as laminated limestone does not have internal lamination but is homogeneous  
422 and without macrofossils. As for laminated limestone beds H32 and H36, it is underlain and  
423 overlain by laminated shale, has sharp planar top and bottom contacts, and has exceptionally  
424 low, slightly negative magnetic susceptibility values. The lowest measured vol MS of  $-0.13$   
425  $\times 10^{-8}$  SI implies, by extrapolating the regression of Fig. 2a (Section 3.b), 97.3 %CaCO<sub>3</sub> and  
426 hence these limestones represent cementation of a primary sediment almost devoid of organic  
427 matter and clay. Partly due to the sharp, planar base Hesselbo & Jenkyns (1995) inferred a  
428 dilute turbidity-current origin for bed H30 (which they named 'Intruder'). However, in the  
429 absence of direct evidence for basal erosion, grading or cross-lamination alternative  
430 explanations for the deposition of almost pure carbonate mud should be considered.

431

#### 432 **4.c. Lateral and stratigraphic variations in limestone proportions**

433 Unlike the marls and laminated shale beds, average limestone bed thicknesses are  
434 consistently close to 10-15 cm at all the logged localities and in every zone of the Hettangian  
435 (Fig. 1b). Hallam (1964; 1986) regarded the consistency in limestone bed thickness of the Blue  
436 Lias, independent of locality and zonal thickness, as indicative of a diagenetic rather than a  
437 primary control on limestone formation. Although average limestone bed thicknesses remain  
438 nearly constant, the proportion of limestone beds by thickness per ammonite zone varies  
439 substantially from place to place and stratigraphically (Fig. 1b). Areas with thinner biozones  
440 (lower net accumulation rate or 'condensed sections') have higher average proportions of  
441 limestone (Fig. 1b, figure 2 of Page, 1995). For example, all four ammonite zones of the  
442 Hettangian of Lyme Regis have a far higher proportion of limestone than those on the West  
443 Somerset coast (Fig. 1b).

444 At Lyme Regis, representing an area of low net accumulation rate, all the zones of the  
445 Hettangian are of similar thickness and the average bed thicknesses for all rock types are also

446 similar in the different zones (Fig. 1b). By contrast, on the West Somerset coast the oldest  
447 zones (Tilmanni and Planorbis) are much thinner than the succeeding (Liasicus and Angulata)  
448 zones; significantly, the large change in zonal thickness there is mirrored by changes in average  
449 bed thickness of the light and dark marls and the laminated shales (Fig. 1b).

450         The association of changes in average non-limestone bed thickness with changing zonal  
451 thickness is interpreted here as indicating a large change in net accumulation rates at the end  
452 of the Planorbis Zone times or start of the Liasicus Zone for sections on the West Somerset  
453 coast. In this study, only the base of the Liasicus Zone was logged at Lavernock (Fig. 3).  
454 However, the much greater thickness of the Liasicus Zone interval at Lavernock compared to  
455 the Tilmanni and Planorbis zones (Waters & Lawrence, 1987; Warrington & Ivimey-Cook,  
456 1995) indicates a similar change in net accumulation rate to that of the West Somerset coast.

457         The Liasicus Zone is consistently associated with lower proportions of limestone than  
458 preceding and succeeding Hettangian zones in different localities (Fig. 1b, Hallam, 1960;  
459 Palmer, 1972). This difference in character has led to member-scale subdivisions of the Blue  
460 Lias Formation with locally applied names i.e. the Lavernock Shales (Richardson, 1905;  
461 Waters & Lawrence, 1987); the St Audries Shales (Palmer, 1972) and the Saltford Shales  
462 (Donovan, 1956; Ambrose, 2001).

463         In the lower Liasicus Zone, higher velocities on downhole sonic logs related to  
464 relatively higher clay content, and higher gamma-ray counts related both to thorium and  
465 potassium in the marls and shales and to uranium within organic matter, allow ready correlation  
466 of this portion of the Blue Lias across Britain (Whittaker, Holliday & Penn, 1985). The base of  
467 this mudrock-dominated interval is diachronous because, in the English Midlands, there is  
468 biostratigraphical evidence that it occurs within the Planorbis Zone (Old, Sumbler & Ambrose  
469 1987; Ambrose 2001), whereas in West Somerset and Lavernock the base is close to the base  
470 of the Liasicus Zone (Figs 3 and 5).

471 Mapping of the oldest strata of the Blue Lias Formation on the London-Brabant  
472 Platform and the Radstock Plateau near Bristol shows that the Liasicus Zone in the Hettangian  
473 and Semicostatum Zone of the Sinemurian were times of accelerated onlap (Donovan, Horton  
474 & Ivimey-Cook, 1979; Donovan & Kellaway, 1984). An inferred sea-level rise during these  
475 zones was suggested by Hallam (1981) and broadly supported by Hesselbo & Jenkyns (1998)  
476 and Hesselbo (2008).

477 At Lyme Regis, in the Liasicus Zone, the zonal thickness and the average thicknesses  
478 of the various rock-types are similar in the overlying and underlying zones, but there is  
479 nevertheless a lower proportion of limestone (Fig. 1b). Therefore, rising sea levels were  
480 apparently associated with reduced probability of limestone formation. The near-constancy of  
481 net accumulation rate at Lyme Regis, as indicated by the near-uniform average bed thicknesses  
482 of the marl and laminated shale, presumably resulted from an underlying tectonic block  
483 maintaining a relatively level sea floor within turbulent-water depths (due to storm winnowing)  
484 despite sea-level rise (Sellwood & Jenkyns, 1975). Apparently, rising sea levels during the  
485 Liasicus Zone times at Lyme Regis led to slight increases in water depth and less probability  
486 of limestone formation, but the increase in accommodation space was too small to allow  
487 substantially increased net sedimentation rates.

488 On the West Somerset coast and at Lavernock, increased accommodation space and  
489 higher sedimentation rates during the Liasicus Zone account for locally greater thicknesses of  
490 mudrocks (i.e. greater zonal thicknesses and greater average thickness of marl and laminated  
491 shale beds) compared to the Tilmanni and Planorbis zones (Figs 1b, 3, 5a). In these localities,  
492 the rapid increase in net accumulation rates apparently resulted from faster, probably fault-  
493 related, subsidence that was coincident with the sea-level rise (i.e. the increased subsidence  
494 rates exaggerated the effect of sea-level rise on local water depths). Fault-related activity is  
495 documented for the Hettangian in the Wessex Basin (Jenkyns & Senior, 1991) and South

496 Glamorgan in South Wales (Wilson et al., 1990) and fault movement occurred at some point  
497 during the Jurassic associated with the Bristol Channel area (Waters & Lawrence, 1987; Bixler,  
498 Elmore & Engel, 1998). Furthermore, fossil methane seeps dating from the Bucklandi Zone in  
499 the Sinemurian might be related to fault movement on the West Somerset coast (Allison,  
500 Hesselbo & Brett, 2008; Price, Vowles-Sheridan & Anderson, 2008).

501         At Southam Quarry near Long Itchington, the majority of the Liasicus Zone strata  
502 consist of laminated shale (Figs 1b and 6). This observation might be thought to indicate that  
503 greater water depth due to sea-level rise in the Liasicus Zone was associated with the conditions  
504 required for the preservation of lamination (especially bottom-water dysoxia and anoxia, cf.  
505 Hallam & Bradshaw, 1979). However, in both West Somerset and Lyme Regis, although there  
506 is a reduction in the proportions of limestone in the Liasicus Zone, unlike Long Itchington the  
507 proportions of laminated shale are lower than in the succeeding Angulata Zone (Figs 1b, 4 and  
508 5a and b; Weedon, 1987a). Hence, it is the formation of a lower proportion of limestones, not  
509 the development of laminated shales, which can be consistently related to rising sea  
510 level/greater water depth.

511

## 512         **5. Intra-formational hiatuses**

513         Weedon (1986; 1987a; 1987b) reasoned that differences between localities in the  
514 numbers of regular sedimentary cycles, thought to result from Milankovitch orbital forcing of  
515 climate, could be explained by the presence of intra-formational hiatuses. Although Hallam  
516 (1960; 1987) disagreed, there are numerous lines of evidence, summarized in the sub-sections  
517 below, for both intermittent sea-floor erosion and for missing stratigraphic intervals within the  
518 offshore Blue Lias Formation of southern Britain.

519

520         ----- Figure 8 near this position -----

521 **5.a. Shaw plot**

522 In Table 1 there are 63 levels in the Hettangian and Lower Sinemurian, out of 130  
523 available, where the same biohorizon level (i.e. biohorizon top or biohorizon base) has been  
524 located to within a few centimetres both at Lyme Regis and on the West Somerset coast. This  
525 stratigraphic refinement allowed construction of the Shaw plot in Fig. 8 that illustrates the  
526 correlation of these two sites. At Lyme Regis, the base of the Angulata Zone lies somewhere  
527 between the lowest level with recorded *Schlotheimia* at 11.06 m (base of bed H84) and the  
528 highest recorded level with *Waehneroceras* at 9.66 m (within bed H71), as indicated by short  
529 horizontal lines in Fig. 8. Using the line of correlation between St Audries and Lyme Regis, its  
530 location has been inferred to be close to 10.54 m (within bed H77 Fig. 4, Table 1) as indicated  
531 using the long grey horizontal arrow in Fig. 8. Alternatively, the line of correlation from  
532 Quantock's Head rather than St Audries Bay, with fewer biohorizon constraints, would imply  
533 that the base of the Angulata Zone lies close to 10.13 m at Lyme Regis (within bed H73).

534 Subzones on the West Somerset coast sections are thicker than those in the  
535 corresponding section at Lyme Regis, as indicated in figures at the bottom of Fig. 8. Treating  
536 the biohorizon picks as time lines, the amount of strata within each interval results from the  
537 combination of the sedimentation rates and the effects of intra-formational hiatuses: i.e. the net  
538 accumulation rate. Shallower slopes on the line of correlation indicate higher net accumulation  
539 rates on the West Somerset Coast relative to the Devon/Dorset coast.

540 In contrast to the Lyme Regis section, on the West Somerset Coast the much thicker  
541 Liasicus and Angulata zones compared to the Tilmanni and Planorbis zones are mirrored by  
542 the increased average thicknesses of the corresponding marl and shale beds (Fig. 1b, Section  
543 4.c). Hence, the major decrease in the average slope of the line of correlation in Fig. 8 at the  
544 base of the Liasicus Zone is interpreted as due to substantially increased net accumulation rates  
545 in West Somerset. In detail, the breaks in slope (nearly horizontal or nearly vertical segments)

546 of the line of correlation are interpreted as due to hiatuses or intervals of exceptionally low  
547 accumulation rate, and have been labelled with the corresponding bed numbers. These breaks  
548 in slope of the line of correlation are discussed in Section 5.c. The breaks in slope are defined  
549 by multiple points, significantly reducing the likelihood that they simply result from mis-  
550 placing the tie-levels due to collection failure for key ammonites.

551

### 552 **5.b. Minor erosion**

553 Several lines of field evidence for minor sea-floor erosion were used by Weedon (1986)  
554 to argue for storm-induced bottom-water turbulence. Protrusive *Diplocraterion* burrow  
555 mottles, which are found only within the limestones and light marls, have been described at all  
556 four localities studied here as well as at Saltford, Avon (Fig. 9c, Sellwood, 1970; Donovan &  
557 Kellaway, 1984; Weedon, 1987a; Mogadam & Paul, 2000; Barras & Twitchett, 2007). Tiering  
558 analysis at Lyme Regis (Mogadam & Paul, 2000) showed that *Diplocraterion* cross-cuts all  
559 other trace fossils except *Chondrites* which is well known to have been produced by late-stage  
560 deposit feeders within anoxic sediments (Bromley & Ekdale, 1984). The observations of  
561 Mogadam & Paul (2000) suggest re-excavation of the vertical U-shaped burrow following  
562 rapid centimetre-scale sediment removal (Seilacher, 2007).

563 At Lyme Regis, dark marl beds that are only a few centimetres thick are locally missing  
564 for several metres laterally (Weedon, 1986). Within limestone bed 23 ('Mongrel') locally a  
565 thin dark marl bed is replaced laterally by centimetre-scale, metre-wide scours filled with  
566 bioclastic packstone. The former presence of a thin bed of dark marl is in some places recorded  
567 by a layer of isolated dark marl burrow mottles within what otherwise appears to be a single  
568 limestone bed (e.g. in bed 19, Fig. 9d). In West Somerset, this phenomenon is occasionally  
569 observed in thick light marl beds but more typically an opposite arrangement occurs with  
570 isolated bands of light burrow-fills within dark marls representing relics of thin light marl beds.



571 Paul, Allison & Brett (2008) also noted that occasional ‘exotic’ sediment fills within uncrushed  
572 ammonites at Lyme Regis could indicate material subsequently removed by erosion.

573 Radley (2008) argued that at Southam Quarry, Long Itchington, erosion within  
574 laminated shale was linked to distal storm influences below normal storm wave-base. He  
575 described siltstone scour-fills within Liasicus Zone laminated shales as well as highly  
576 elongated limestone nodules containing imbricated ammonites, which were interpreted as  
577 gutter casts. The scour fills are associated with a trace fossil indicative of a crustacean escape  
578 structure and therefore very rapid deposition (Radley, 2008; O’Brien, Braddy & Radley, 2009).  
579 Similar presumed scour fills, full of ammonites and shell fragments, within light marl beds are  
580 also known in West Somerset, albeit mainly in the Planorbis Subzone (e.g. bed 24).

581 A scour fill at Lyme Regis in the top of a limestone bed, probably from the Rotiforme  
582 Subzone, Bucklandi Zone, consists of a shallow depression around 50 cm across filled with  
583 coarse shelly debris and abundant small articulated echinoids (?*Diademopsis*) and common  
584 articulated ophiuroids (Page collection, Bristol City Museum and Art Gallery). These  
585 echinoderms retained their articulation due to rapid burial, presumably as waning storm-  
586 currents deposited previously suspended sediment. A second level with common, but more  
587 scattered *Diademopsis* in laminated mudstone bed 17 (Planorbis Zone and Subzone) near  
588 Watchet, West Somerset, may indicate a similar event, although there is no equivalent  
589 concentration of shelly debris (K. N. P. pers. obs. 2015).

590 Found commonly throughout the sections on the Devon/Dorset and West Somerset  
591 coast are centimetre-scale horizons with: a) concentrated bivalve fragments; b) lenses of  
592 echinoid debris; c) abundant large ammonites on the surface or base of limestone beds, and/or  
593 d) scattered large ammonites and nautiloids with encrusting oysters and/or crinoid debris on  
594 the tops of limestone beds. Some of these features have been previously recorded by Paul,  
595 Allison & Brett (2008) and they indicate either periods of increased sea-floor turbulence that

596 led to winnowing of fines, fragmentation of shells and the concentration of bioclasts or periods  
597 of very slow, or halted deposition. In the latter case, epifauna such as oysters and crinoids had  
598 time to attach to the ‘benthic islands’ created by large shells. Such observations can coincide  
599 with additional evidence for significant intervals of missing strata.

600

### 601 **5.c. Major hiatuses**

602 The following sub-sections summarize the Shaw plot and field evidence for significant  
603 hiatuses at many levels within the Hettangian and Lower Sinemurian offshore facies of the  
604 Blue Lias of southern Britain. Note that in some cases these major hiatuses can be potentially  
605 linked to sea-level rises and in others to sea-level falls.

606

#### 607 **5.c.1. Tilmanni and Planorbis zones, Hettangian**

608 A widespread, diachronous erosion surface across southern Britain at the base of the  
609 Blue Lias Formation has been explained in terms of latest Triassic sea-level fall followed by a  
610 rise in the earliest Jurassic (Tilmanni Zone, Donovan, Horton & Ivimey-Cook, 1979; Hallam,  
611 1981; 1997; Wignall, 2001; Hesselbo, Robinson & Surlyk, 2004). In the Bristol area at several  
612 localities (Filton railway cutting, Chipping Sodbury, Henleaze, Wick and Doynton), Donovan  
613 & Kellaway (1984) recorded Johnstoni Subzone (i.e. upper Planorbis Zone) strata directly on  
614 top of the ‘Pre-planorbis Beds’ (i.e. the Tilmanni Zone). Widespread condensation by  
615 winnowing of mud-grade sediment during the Tilmanni and Planorbis zones apparently led to  
616 numerous centimetre-scale horizons of small bivalve fragments and closely spaced limestone  
617 beds at Lyme Regis, West Somerset Coast, and Lavernock (Kent, 1937; Hallam, 1960;  
618 Hesselbo & Jenkyns, 1995; 1998). Furthermore, Kent (1937) noted limestone intraclasts  
619 encrusted by serpulids as well as borings, indicative of sea-floor erosion and non-deposition,

620 within the Tilmanni and/or Planorbis zones of Nottinghamshire (the precise stratigraphic levels  
621 not being reported).

622 The apparent thinness of the *Neophyllites*-bearing levels at the base of the Planorbis  
623 Subzone (biohorizons Hn3 and Hn4, bed 9 of Whittaker & Green, 1983), suggests that there is  
624 condensation at this level in West Somerset (Page, 1995; Bloos & Page, 2000a). This  
625 supposition is confirmed by a corresponding break in slope in Fig. 8. A similar break in slope,  
626 implying a gap in the West Somerset coast section, occurs at the base of the Johnstoni Subzone  
627 (bed 25). A break in slope associated with bed 25 is also found on a Shaw plot of the West  
628 Somerset coast versus Lavernock (Table 1 data, not illustrated). Currently, there is no  
629 independent biostratigraphical evidence for a gap at this level on the West Somerset coast but,  
630 as noted in Section 5.b, presumed scour fills are present in bed 24.

631

### 632 **5.c.2. Liasicus Zone, Hettangian**

633 Liasicus Zone strata have not provided much field evidence for stratigraphic gaps.  
634 Radley (2008) noted in Southam Quarry, near Long Itchington, the presence of limestone  
635 nodules encrusted by serpulids and oysters (*Liostrrea*) with scratches and grooves attributed to  
636 crustaceans. This evidence certainly indicates sea-floor exhumation of the nodules and a period  
637 of non-deposition (though this might have been short-lived). He inferred an Angulata Zone  
638 age, assuming causal factors such as lowered sea level rather than sediment starvation.  
639 However, comparison of the stratigraphic level shown (figure 5 of Radley, 2008) for the  
640 encrusted nodules with Fig. 3, combined with the biostratigraphy of Clements *et al.* (1975;  
641 1977), indicates that this erosion and non-deposition occurred during the Liasicus Zone.

642 Breaks in slope in Fig. 8 indicate possible hiatuses within the Liasicus Zone at Lyme  
643 Regis associated with unnamed limestone beds H58 and H68. Consistent with increased  
644 bottom-water turbulence, if not direct evidence for non-deposition, is the presence of abundant

645 macroconch *Waehneroceras* commonly with encrusting *Liostrea* on the top surface of bed H58,  
646 as well as lenses of echinoid debris, especially spines in a few centimetres of the overlying  
647 marl. Figure 8 also indicates a stratigraphic gap at the base of bed 67 at the base of the Laqueus  
648 Subzone on the West Somerset Coast. Two metres below bed 67, the top of bed 65 (Fig. 5a)  
649 also yields common macroconch *Waehneroceras*.

650 Hence, there was apparently increased bottom-water turbulence at the end of the  
651 Portlocki Subzone and beginning of the Laqueus Subzone in both relatively slowly and  
652 relatively quickly subsiding areas. Since bed H68 at Lyme Regis and beds 65 to 67 on the West  
653 Somerset coast occur at the levels of increased MS (Section 3.b), the mid-Liasicus increase in  
654 bottom-water turbulence was apparently associated with a change in sediment composition.  
655 Sequence stratigraphic analysis of the marginal facies in Glamorgan (Section 4.a) led Sheppard  
656 (2006) to infer a major flooding surface in the mid Liasicus Zone – consistent with the analysis  
657 by Hesselbo & Jenkyns (1998) of coeval marine strata from across Britain.

658

### 659 **5.c.3. Angulata Zone, Hettangian**

660 Correlation of a downhole log from the borehole at Burton Row in north Somerset, 20  
661 km north east of Quantock's Head (Fig. 1a), with the lithological log of Weedon (1987a) from  
662 the Devon coast suggested to Smith (1989) that a gap exists in the Angulata Zone at Lyme  
663 Regis. Deconinck *et al.* (2003) inferred, using kaolinite/illite ratios from the West Somerset  
664 coast, that a stratigraphic gap occurs at Lyme Regis at the top of the Angulata Zone. Hesselbo  
665 & Jenkyns (1995; 1998) also argued for condensation and thus reduced accumulation rates in  
666 the middle Angulata Zone at Lyme Regis, as indicated by the unusually close spacing of  
667 limestone beds and nodule-bearing horizons (e.g. bed 1 or 'Brick Ledge').

668 Figure 8 confirms the presence of stratigraphic gaps in the Angulata Zone at Lyme  
669 Regis with at least at one level in the Complanata Subzone (bed 1c within 'Brick Ledge') and

670 at two levels within the Depressa Subzone (bed 7c or ‘Lower Skulls’, and bed 17 or ‘Upper  
671 White’). The Shaw plot also indicates a gap at bed 134 in the Depressa Subzone on the West  
672 Somerset coast (Fig. 8), a level characterized by abundant large macroconch ammonites  
673 (*Schlotheimia*), again suggesting low net accumulation rates.

674

675 ----- Figure 9 near this position -----

#### 676 **5.c.4. Bucklandi Zone, Sinemurian**

677 Direct evidence for erosion at Lyme Regis during the Conybeari Subzone, Bucklandi  
678 Zone, is provided by a limestone intraclast with the size and shape reminiscent of a small  
679 limestone nodule, but found *in situ* within limestone bed 25 (‘Top Copper’, Fig. 9a, Weedon,  
680 1987a). The intraclast surface has the characteristics of a hardground as it is bored both by  
681 bivalves (possible *Lithophaga* crypts, Fig. 2.5e of Weedon, 1987a) and by *Talpina ramosa* Von  
682 Hagenow (150–250 µm diameter, possibly made by phoronids). The intraclast surface is  
683 encrusted by at least two generations of *Liostrea*, which also have *Talpina ramosa* borings  
684 (Figs 9ai and aii). The intraclast surface is directly overlain by an unusual packstone of small  
685 gastropods, benthic foraminifera and larger bivalve fragments and succeeded by normally  
686 bioturbated wackestone. Thus, it appears that a period of increased turbulence led to  
687 exhumation of a limestone nodule, exposure for sufficient time for repeated colonization and  
688 boring (over at least two years based on the two or three generations of bivalves), followed by  
689 burial whilst the turbulence was sufficient to lead to generation of the packstone (i.e. grain-  
690 supported fabric) before a return to typical carbonate mudstone and wackestone deposition.

691 There is no biostratigraphic evidence for missing strata at the level of bed 25 at Lyme  
692 Regis containing the limestone intraclast (Fig. 9a). However, large ammonites are common in  
693 the limestone bed 153 on the West Somerset coast, which correlates biostratigraphically with  
694 bed 24 at Lyme Regis (i.e. Biohorizon Sn3b with *Metophioceras* ex grp *rouvillei* (Reynès),

695 etc). In Fig. 8, the kink in the line of correlation at the level of bed 153 (at about 81.5 m)  
696 indicates condensation of the West Somerset section relative to Lyme Regis. Hence,  
697 erosion/non-deposition was apparently simultaneous at Lyme Regis and on the West Somerset  
698 coast during the middle part of the Conybeari Subzone. The break in slope of the line of  
699 correlation was determined more by sediment condensation at the level of bed 153 in West  
700 Somerset than by erosion associated with beds 24 and 25 at Lyme Regis.

701 In bed 29 at Lyme Regis ('Top Tape', Fig. 4), also within the Conybeari Subzone,  
702 Hallam (pp8–9, 1960) noted the presence of glauconite, both as discrete 'granules' and in  
703 microfossil infills, this mineral being an indicator of reduced accumulation rate (Odin &  
704 Matter, 1981). At beach level on either side of Seven Rock Point, west of Lyme Regis, bed 29  
705 forms a prominent ammonite 'pavement' covered with large specimens of *Metophioceras* ex  
706 grp. *conybeari* (J. Sowerby) (Sn5b *conybeari* Biohorizon: Page 2002, 2010b; 2010c), and this  
707 is matched by its correlative bed 161 in West Somerset, which has the same group of species  
708 in abundance on its base. The equivalent level is also recognizable palaeontologically near  
709 Pilton in north Somerset (pers. obs. by K.N.P., 1992) and correlates with the Calcaria Bed in  
710 the Bristol-Bath area where the widespread evidence for truncation, condensation and  
711 phosphatization of fossils has been specifically attributed to shallowing (Kellaway & Donovan,  
712 1984). Figure 2 of Page (1995) clearly illustrates, for the Hettangian/Sinemurian boundary  
713 interval of the West Somerset Coast, Lyme Regis area and Saltford Cutting near Bristol, the  
714 way that lateral loss and condensation of biohorizons is associated with an increased proportion  
715 of limestone compared to marl and shale.

716 A widespread late Angulata–early Bucklandi erosive phase is also indicated by the non-  
717 sequences and condensation at this level described in eastern France, southern Germany and  
718 Austria, contrasting with the relative completeness of the Sinemurian GSSP section on the  
719 West Somerset coast (Page *et al.*, 2000; Bloos & Page, 2002). An indication for shallowing at

720 this time is also provided in South Wales near Cardiff where typical offshore Blue Lias of Unit  
721 A of the Porthkerry Formation in the Angulata Zone is overlain by the near-shore Unit B facies  
722 (i.e. limestone dominated and lacking laminated shales and laminated limestones, Section 4.a).  
723 Unit B and C facies are, in turn, overlain by uppermost Angulata Zone and Bucklandi Zone  
724 oolitic marginal facies suggesting further shallowing (Waters & Lawrence, 1987; Wilson et al,  
725 1990).

726 In the Cardiff area, the Porthkerry Formation with Bucklandi and Semicostatum Zone  
727 ammonites is found on top of a bored surface on the oolitic marginal facies (Waters &  
728 Lawrence, 1987). Similarly, near Southerndown Porthkerry Formation Unit D of the same  
729 zones (normal offshore Blue Lias with about 60 % nodular limestones and marls) occurs on  
730 top of marginal facies (Wilson et al., 1990). The nature of these successions is consistent with  
731 a rise in relative sea level at the end of the Bucklandi Zone.

732

### 733 **5.c.5. Early Semicostatum Zone, Sinemurian**

734 As reviewed by Donovan & Kellaway (1984, e.g. their figures 5 and 6), a non-  
735 conformity in the Bristol area is overlain by phosphatised sediments and fossils with truncation  
736 of the Bucklandi Zone and successive overstepping of all the Hettangian biozones and the  
737 Rhaetian onto the Radstock Plateau to the south (i.e. approaching the Carboniferous Limestone  
738 massif of the Mendip Hills).

739 As evidence for coeval erosion and condensation at Lyme Regis, Hallam (1960)  
740 illustrated the truncation of a *Diplocraterion* burrow, and noted glauconite and phosphate  
741 associated with bed 49 ('Grey Ledge'). This level is now known to be associated with up to  
742 four missing biohorizons from the top of the Bucklandi Subzone to the base of the  
743 Scipionianum Subzone, within the lower part of the Semicostatum Zone (Page, 2003, 2010b;  
744 2010c). Additionally, on the Devon/Dorset coast, Gallois & Paul (2009) showed that there are

745 lateral variations in the amount of strata removed at this level from the uppermost Blue Lias  
746 Formation and that locally there is a bored surface on bed 49 and, throughout the area, deep  
747 *Diplocraterion* burrows are present, commonly at more than one level in beds 47–49. It should  
748 be noted, however, that the ammonite faunas recorded through this interval indicate that these  
749 levels may be of slightly different ages in different places and hence what are termed beds 47,  
750 48 or 49 in different places may not be exactly the same lithostratigraphical entities. Hallam  
751 (1981) linked the change in facies above bed 49 to both the accelerated onlap on the London  
752 Platform described by Donovan, Horton & Ivimey-Cook (1979) and to sea-level rise.

753         There is no evidence for a break in sedimentation in the late Bucklandi to basal  
754 *Semicostatum* zones on the West Somerset coast where the biohorizon succession appears to  
755 be complete. Interestingly, however, there is a concentration of ammonites at the level of bed  
756 247 of Whittaker & Green (1983) in the Lyra Subzone (Page 1992; 2009, biohorizon Sn 15b  
757 of Page, 2010b), which may indicate at least one phase of reduced accumulation rates in the  
758 early *Semicostatum* Zone. There are several levels in the 5–6 m of shale-marl/limestone  
759 alternations, below which are concentrations of shelly debris, with common large ammonites,  
760 and one prominent level of *Diplocraterion* burrows in bed 242 (K.N.P. pers. obs. 2013–2015).  
761 Notably, the ammonite fauna of bed 247 (e.g. *Paracoronicerias ex grp charlesi* Donovan) is  
762 very close in terms of biohorizonal assignment to that recorded from the top c. 6–10 cm of bed  
763 49 at the ‘Slabs’, between Axmouth and Lyme Regis (Page, 2002), immediately below the non-  
764 sequence and with *Scipionianum* Subzone strata immediately above. The lower part of bed 49,  
765 however, still appears to belong the Bucklandi Subzone (and Zone) because large *Arietites* are  
766 common.

767

## 768         **6. Preservation of ammonites**



769           It has long been believed that since the macrofossils, especially ammonites and  
770 nautiloids, are largely uncrushed, and horizontal sections of burrow mottles are nearly circular  
771 in limestone beds of the Blue Lias Formation, cementation must have started prior to significant  
772 compaction, and hence was both early and at shallow depth (Kent, 1936; Hallam, 1964;  
773 Weedon 1987a; Arzani, 2006; Paul, Allison & Brett, 2008). Since the uncrushed ammonite and  
774 gastropod shells in the limestones would have originally been aragonite, the cementation must  
775 also have pre-dated dissolution or inversion to calcite.

776           At Lyme Regis, ammonites completely enclosed within limestone beds typically have  
777 their originally aragonitic shells replaced by sparry calcite and the inner and outer whorls are  
778 uncrushed. By contrast, ammonites diagenetically ‘welded’ onto the surfaces of such beds  
779 usually present an uncrushed internal mould of the outer whorls with the shell entirely absent.  
780 Importantly, their inner, septate whorls are represented predominantly by an external mould on  
781 the surface of the limestone bed.

782           This differential preservation according to the location of the ammonite specimens can  
783 be explained by the carbonate cementation generating a framework-supporting fabric that  
784 formed first at the centres of (i.e. mid-way through) what became the limestone beds. When  
785 and where the cementation and framework support occurred before aragonite dissolution, the  
786 full three-dimensional shape of the aragonitic ammonite shell was preserved, allowing for a  
787 later sparry calcite replacement and infill. However, on the outer margins of limestone beds,  
788 cementation and framework support appears to have been later than aragonite dissolution,  
789 albeit before significant compaction. Consequently, although this later cementation could  
790 preserve the three-dimensional shape of the shell where already filled with marl (in the body  
791 chamber and, in some cases, perforated sections of the phragmocone), it could not preserve the  
792 thickness of the shell or support inner whorls that lacked internal sediment. Arzani’s (2006)

793 study of the limestone micro-fabrics also showed that, despite the typically uncrushed nature  
794 of the macrofossils, cementation of the edges of the limestones did occur during compaction.

795         Although a cursory examination of the Devon–Dorset and West Somerset sections may  
796 give an impression that ammonites do not occur in every limestone bed, they have been  
797 recorded at far more levels than noted by Paul, Allison & Brett (2008) at Lyme Regis (Page,  
798 2002). Ammonites are common only in certain beds but prolonged examination over many  
799 years by K.N.P. has led to the recovery of very rare isolated specimens from many levels  
800 throughout the Devon–Dorset and West Somerset coastal successions. The simplest  
801 explanation for the apparent lack of ammonites within some limestone beds at Lyme Regis is  
802 preservation failure caused by cementation following a combination of aragonite dissolution,  
803 burrowing and compaction that destroyed all trace of the shells. Which leads to the critical  
804 question: why do some limestones record cementation before aragonite dissolution and others  
805 do not? This issue is re-visited in Section 8.

806         Paul, Allison & Brett (2008) suggested that the apparent lack of dissolution and  
807 encrustation of uncrushed ammonite and nautiloid shells within limestone beds, given the  
808 average bed thickness, implies much more rapid sedimentation of these lithologies than the net  
809 rate for the formation as a whole. As evidence for rapid sedimentation, they cited the presence  
810 of ammonite shells preserved in a near-vertical orientation within limestone beds, as well as  
811 cases of ammonite imbrication. However, their observations were primarily based on bed 41  
812 (‘Best Bed’, Bucklandi Zone), which has abundant small ammonites (including *Vermiceras*  
813 *scylla* (Reynès)) that would have been readily re-oriented by large burrowers. Just two  
814 additional beds in the Johnstoni Subzone in the Planorbis Zone have common small ammonites.  
815 Otherwise the limestone beds typically have a large-bodied ammonite fauna.

816         In addition, although encrustation on ammonites appears to be mainly observed on the  
817 surfaces of limestone beds, its reported absence from specimens *within* limestone beds (Paul,

818 Allison & Brett 2008) is not necessarily evidence for rapid sedimentation because biologically  
819 relevant factors may have been influential. In fact, the benthic macrofauna of the limestone  
820 beds is commonly characterized by low diversity and locally high density, indicative of either  
821 a ‘high-stress’ environment or opportunistic colonization during brief periods of ‘improved’  
822 conditions. For example, rhynchonellid brachiopods dominate bed 11 and the tops of beds 19  
823 and 23 at Lyme Regis, beds 147 and 151 on the Somerset Coast and bed 21c at Long Itchington,  
824 whereas *Gryphaea* dominates at the tops of bed 13 and beds 14 to 17 and 31 at Lyme Regis  
825 and at the tops of beds 136 and 138 on the Somerset Coast. It is likely that these controls on  
826 benthic colonization were due to intermittent bottom-water dysoxia which would have also  
827 inhibited encrustation of ammonites. There are some exceptions to these general observations,  
828 however, as there is evidence that some of the rhynchonellid brachiopods may have inhabited  
829 *Thalassinoides* burrows preferentially. Additionally, occasional winnowing may have  
830 concentrated some of the shelly material, for instance in bed 31 at Lyme Regis. At this latter  
831 level, *Gryphaea* apparently show current sorting as they are dominated by the larger, heavier  
832 lower valve in random orientations throughout the bed – possibly indicative of rapid deposition  
833 after a storm (C. R. C. Paul, pers. comm. 2016).

834         In the light and dark marls and the black laminated shales, without the early cementation  
835 of the limestones, the aragonitic fossils were much less likely to be preserved and hence subject  
836 to compaction and early diagenetic dissolution. At Lyme Regis in particular, ammonites are  
837 absent from most of the light and dark marls, but in some of the laminated shales very poorly  
838 preserved shell-less impressions can sometimes be found. Scattered oyster xenomorphs in the  
839 marls, however, prove that ammonites were once present (Paul, Allison & Brett 2008).  
840 Dissolution of aragonite and bioturbation and hence destruction of any remaining trace of shell  
841 can be assumed to have removed most of the ammonites from such levels, especially when no

842 traces of other aragonitic shells, such as bivalves, are observed (Wright, Cherns & Hodges,  
843 2003).

844 In West Somerset, however, the situation is more complex. White aragonitic shells  
845 persist in laminated shales through much of the succession, although they are only well  
846 preserved and iridescent at certain levels in the Planorbis and middle Liasicus zones. By  
847 analogy with calcareous nannofossil preservation (Section 4.b), the preservation of iridescent  
848 aragonite is likely to be connected to the high organic-carbon contents of the laminated shales,  
849 as has proven to be the case in other Jurassic shale sequences from the British Isles (e.g. Hall  
850 & Kennedy, 1967; Hudson & Martill, 1991).

851 Commonly, on the West Somerset coast in the laminated shales and especially in the  
852 marls, only an impression of the shell remains, picked out by a residual brown organic film:  
853 the remains of the organic content of the shell, in particular the periostracum. This pattern of  
854 preservation indicates that the aragonite dissolution post-dated the end of bioturbation in the  
855 marls. In the upper Bucklandi and Lyra subzones, levels with white aragonite preservation can  
856 pass laterally into areas with brown calcitic shell preservation as major faults are approached.  
857 In such cases, the inversion of aragonite to calcite in the marls and shales is clearly associated  
858 with the circulation of fluids along such faults, for instance during the tectonic inversion of the  
859 basin, as described by Bixler, Elmore & Engel (1998). At some levels, both brown calcitic and  
860 white aragonitic shells may also contain pyrite, commonly associated with specific layers in  
861 the shell.

862 In the Burton Row borehole in North Somerset, pristine iridescent aragonite is  
863 characteristic of the laminated shales of most of the Hettangian and Sinemurian succession. On  
864 the coast, inversion to brown calcite (e.g. in parts of the Liasicus and Semicostatum zones) was  
865 due to the effects of fluids and/or raised temperatures generated during tectonic inversion  
866 (Water & Lawrence, 1983; Bixler, Elmore & Engel, 1998), whereas conversion of iridescent

867 aragonite in the laminated shales to white and powdery aragonite was probably due to near-  
868 surface weathering and/or the effects of ground-water penetration.

869

870 ----- Figure 10 near this position -----

## 871 **7. Oxygen and carbon isotopes and timing of limestone formation**

### 872 **7.a. Lyme Regis**

873 Figures 2b and 10a show that, at Lyme Regis, oxygen isotopes in the centres of the  
874 limestone beds are as high as -1.5 ‰ VPDB with carbon-isotope values close to 0.0 ‰ VPDB.  
875 These values are not much lighter than the isotopes of unaltered benthic bivalve (*Gryphaea*)  
876 calcite (Weedon, 1987a). Hence, carbon and oxygen isotopes of the Blue Lias, combined with  
877 the near-absence of evidence for compaction of macrofossils, have long been considered  
878 consistent with early cementation (Campos & Hallam, 1979; Gluyas, 1984; Weedon, 1987a;  
879 Arzani, 2006; Paul, Allison & Brett, 2008). The decreases of oxygen-isotope values towards  
880 the edges of limestone beds, where calcium carbonate contents are lower, are consistent with  
881 cementation occurring progressively during the early stages of compaction (Gluyas, 1984;  
882 Weedon, 1987a; Arzani, 2006; Paul, Allison & Brett, 2008). Disseminated framboidal and  
883 euhedral pyrite found throughout the limestones and the non-ferroan nature of the calcite  
884 microspar indicate at least some carbonate generation during sulphate reduction (Gluyas,  
885 1984).

886 Raiswell (1988) postulated that cementation of the Blue Lias limestone beds and  
887 nodules was associated with anaerobic methane oxidation by sulphate within the sulphate  
888 reduction zone. Both normal sulphate reduction and anaerobic methane oxidation generate  
889 carbonate that neutralizes the acidity produced during the precipitation of iron monosulphide  
890 and pyrite oxidation (Raiswell, 1988; Bottrell & Raiswell, 1989). Since there is a restricted  
891 depth interval involved, anaerobic methane oxidation was used by Raiswell (1988) to explain

892 Hallam's (1964) observations of the limited range of limestone bed thickness. In particular,  
893 Raiswell's model requires that shallow cementation (<1 m burial) occurred during a pause in  
894 sedimentation.

895         Bottrell & Raiswell (1989) further demonstrated that pyrite formation occurred over a  
896 longer period in the limestones than in the light marl and dark marls. To explain the sulphur-  
897 isotope composition of the pyrite in the limestones they invoked incorporation of sulphur  
898 derived from the bioturbational oxidation of previously formed pyrite. Such a process implies  
899 limestone cementation close to the zone of burrowing and hence not greatly below the  
900 sediment-water interface.  $\delta^{13}\text{C}$  of carbonate from sulphate reduction or aerobic methane  
901 oxidation is typically less than -10.0 ‰ VPDB. Bottrell & Raiswell (1989) explained the  
902 relatively heavy carbon-isotope values of around 0.0 ‰ VPDB in the limestones as indicating  
903 that the bulk of the carbonate was derived from dissolution of aragonite and high-Mg bioclasts.  
904 Later authors concurred with this suggested source of carbonate (Wright, Cherns & Hodges,  
905 2003; Arzani, 2004; 2006; Paul, Allison & Brett, 2008). Some limestone beds at Lyme Regis  
906 contain centimetre-scale cracks partly filled with bioclastic sediment, indicating that  
907 cementation and fissuring occurred close enough to the sediment-water interface to allow  
908 access to unconsolidated material, presumably following a phase of sea-floor erosion (Hesselbo  
909 and Jenkyns, 1995).

910         Plots of isotope ratios in the Blue Lias Formation show measurements lying near a  
911 trend-line that slopes from near the origin down towards more negative oxygen- and carbon-  
912 isotope ratios. Trends in isotope composition from heavier oxygen isotopes at the centres of  
913 nodules to lighter oxygen isotopes at the edges (Fig. 10, Weedon, 1987a, Arzani, 2006)  
914 apparently confirm the supposition that oxygen isotopes became lighter through time, most  
915 likely due to increasing pore-water temperatures. However, the carbon isotopes in limestone  
916 nodules can increase rather than decrease towards the outside of nodules and consequently do

917 not lie along the main trend of measurements at Lyme Regis (Fig 10a) and West Somerset (Fig.  
918 10c).

919 Assuming that oxygen-isotope values only decreased during the diagenesis of the Blue  
920 Lias Formation, an explanation is needed for why the limestone beds can have average  
921 carbonate with  $\delta^{18}\text{O} = -4.5$  and  $\delta^{13}\text{C} = -1.5$  ‰ VPDB while limestone nodules can have average  
922 carbonate with the same  $\delta^{18}\text{O}$ , but  $\delta^{13}\text{C} = -3.0$  ‰ VPDB (Fig. 10a). The key to this problem is  
923 to regard the main trend in the isotopes in the limestone beds as indicating a mixing line  
924 between the composition of early and late carbonate rather than as a time series.

925 It is now recognized that early meniscus calcite cement associated with carbonate  
926 nodule formation could have provided a supporting framework that allowed the bulk of  
927 cementation to occur much later during compaction (Curtis *et al.*, 2000; Raiswell & Fisher,  
928 2000). This model helps explain why it is so rare to find shallow limestone nodules forming in  
929 modern organic-rich marine sediments (Raiswell & Fisher, 2000). In the Blue Lias Formation,  
930 the very early cement in the limestones with oxygen and carbon isotopes relatively close to 0.0  
931 ‰ VPDB was apparently sufficient to prevent the compaction of large macrofossils. At a later  
932 phase of diagenesis, once compaction had started in earnest, the remaining pore spaces within  
933 the limestone beds could then be partly filled with carbonate that had much lighter oxygen and,  
934 typically also lighter carbon isotopes. This model means that, if cemented relatively quickly,  
935 limestone nodules can show progressive changes in isotopes that, unlike the limestone beds,  
936 record a snapshot of the history of changing pore-water isotopic composition in concentric  
937 zones (including pore-water carbon isotopes becoming heavier while oxygen isotopes became  
938 lighter). Although Arzani (2006) demonstrated that microspar growth was displacive, the  
939 cementation cannot have continued much beyond the end of occlusion of the pore spaces  
940 because the limestone beds and nodules have oxygen isotopes not lighter than about -6.0 ‰.

941 At Lyme Regis, the oxygen isotopes of the calcite microspar in the light and dark marls  
942 and the black laminated shale (-3.5 to -6.0 ‰ VPDB) are much lighter on average than the  
943 limestone beds (Fig. 10a). Hence, the marls and shales appear to have been cemented later than  
944 the limestone beds. However, one sample of light marl from mid-way through bed 15c (BL307,  
945 Table 3B of Weedon, 1987a, Figs 2b and 10a) with %CaCO<sub>3</sub> = 38.2 and %TOC = 0.61 has an  
946 oxygen-isotope value that is far heavier ( $\delta^{18}\text{O} = -1.99$  ‰ VPDB) than the other marl and shale  
947 samples. This sample is interpreted to represent light marl that was cemented by early meniscus  
948 cement, as though destined to become the centre of a limestone bed or nodule, but the amount  
949 of cement was apparently insufficient to provide enough framework support to prevent  
950 compaction during burial.

951 Ferroan and non-ferroan calcite beef occurring near the bases of some laminated shales  
952 at Lyme Regis with  $\delta^{18}\text{O}$  less than -6 ‰ (Campos & Hallam, 1979), not shown in Fig. 10a,  
953 probably formed as a result of over-pressuring during deep burial (Marshall, 1982).

954

### 955 **7.b. West Somerset Coast**

956 Unaltered carbonate of *Liostrea* from the Tilmanni Zone of the West Somerset Coast  
957 have generally much heavier carbon isotopes (+1.6 to +3.9 ‰, Fig. 10c, van de Schootbrugge  
958 *et al.*, 2007) than those found in *Gryphaea* from the Angulata and Bucklandi Zones at Lyme  
959 Regis (+0.5 to +2.5 ‰ VPDB, Figs 2b and 10b, Weedon, 1987a). Korte *et al.* (2009) measured  
960  $\delta^{13}\text{C}$  of between +1.5 and +5.0 ‰ VPDB for *Liostrea* in the Tilmanni Zone of Lavernock (not  
961 shown) with progressively lighter average values in the upper part of the Tilmanni, Planorbis  
962 and lower Liasicus zones. The different ranges of values in the Tilmanni and the Angulata–  
963 Bucklandi zones have been related to secular trends in carbon isotopes within the Hettangian  
964 rather than diagenetic factors (Korte *et al.*, 2009). However, all three groups of measurements  
965 of unaltered benthic bivalve calcite indicate  $\delta^{18}\text{O}$  between about 0.0 and -2.0 ‰ VPDB.



966           The limestones on the West Somerset Coast with  $\delta^{18}\text{O} = -4.0$  to  $-12.5$  ‰ VPDB have  
967 far lighter oxygen isotopes than those at Lyme Regis (compare Fig. 10a with Figs 10b and 10c).  
968 The isotopically lightest values from a limestone bed (Fig. 10b) are derived from beds  
969 associated with mud volcanoes developed in the Bucklandi Zone strata near Kilve (Cornford,  
970 2003; Allison, Hesselbo & Brett, 2008; Price, Vowles-Sheridan & Anderson, 2008). Isotope  
971 values from material described as comprising the mud volcano mounds themselves (i.e.  
972 breccia, 'tufa', crust etc) have been excluded from Fig. 10b.

973           Oxygen isotopes from limestone beds from the Tilmanni and Planorbis Zones on the  
974 West Somerset Coast are not only lighter than the limestone beds at Lyme Regis, but also  
975 generally lighter, rather than heavier, than their associated marls and black laminated shales  
976 (Fig. 10c, Arzani, 2004). The much lighter oxygen isotopes suggest that the limestones were  
977 cemented later than the marls and shales. Nevertheless, large macrofossils within the limestone  
978 beds of the West Somerset Coast are preserved uncrushed in the same manner as observed at  
979 Lyme Regis. Accordingly, cementation started prior to compaction. These apparently  
980 conflicting interpretations can be reconciled if it is hypothesised that the West Somerset Coast  
981 limestone beds had an early framework cement with oxygen isotopes close to 0.0 ‰ VPDB  
982 that was joined by carbonate formed much later that had much lighter oxygen-isotope values.  
983 Thus, the marls and laminated shales became fully compacted and fully cemented at a time  
984 when there remained framework-supported pores within the limestone beds still available for  
985 later cementation by calcite with very light oxygen-isotope values.

986           Campos & Hallam (1979) explained their observations of much heavier average oxygen  
987 isotopes in the limestones of the Lower Jurassic of Devon/Dorset compared to the Lower  
988 Jurassic of the Yorkshire Coast in terms of net sedimentation rate. Their explanation is followed  
989 here with respect to the comparison of the West Somerset with the Devon/Dorset coast,  
990 assuming that the total time for cementation was approximately the same in both cases. In both

991 areas, cementation appears to have started very early, but the limestones at Lyme Regis were  
992 buried more slowly and so their final carbonate was probably precipitated at relatively low  
993 temperatures (overall oxygen isotopes heavier than the marls and shales). The more rapidly  
994 buried limestone beds on the West Somerset Coast apparently ceased full cementation at much  
995 greater depths and thus were formed from pore waters with higher temperatures (overall  
996 oxygen isotopes lighter than the marls and shales).

997 A prolonged cementation history on the West Somerset Coast is indicated by very  
998 negative  $\delta^{18}\text{O}$  in vein calcite (-9 to -12 ‰ VPDB - not shown in Fig. 10), probably associated  
999 with Late Jurassic to Early Cretaceous extensional and Cenozoic compressional faulting  
1000 (Bixler, Elmore & Engel, 1998).

1001

## 1002 **8. Synthesis**

1003 In the offshore facies, at the scale of ammonite zones, lateral and stratigraphic variations  
1004 in the characteristics of the Blue Lias Formation are not due to variations in the composition  
1005 of specific rock types. Neither the water depth nor the net accumulation rate influenced the  
1006 average composition of the rock type (Fig. 1c), a conclusion that follows from the hemipelagic  
1007 origin of the sediment (Section 4.b). The key variables determining the characteristics of the  
1008 Formation are: a) the average thicknesses of beds of light marl, dark marl and black laminated  
1009 shale; and b) the proportion of limestone.

1010 Variations in the average thickness of the marls and shales are associated with  
1011 variations in zonal thickness and were determined by the net accumulation rate (Section 4.c).  
1012 The uniformly and relatively thin zones of the Hettangian at Lyme Regis are associated with  
1013 thin beds of marls and shales. On the West Somerset Coast, the younger stratigraphically  
1014 thicker zones are associated with thicker beds of marls and shales whose deposition post-dated

1015 a major increase in accumulation rate at the start of the Liasicus Zone (Figs 1b and 8, Section  
1016 4.c).

1017 On the scale of ammonite zones, the proportion of limestones was linked to the net  
1018 accumulation rate as determined by rates of subsidence and sea-level variations. The abundant  
1019 evidence for intra-formational hiatuses and evidence for storm-related scours and winnowing  
1020 episodes (Section 5) are consistent with the overall deposition of fines limited by the storm  
1021 wave base. Raiswell's (1988) model for the formation of limestone nodules and beds within a  
1022 restricted interval of anaerobic methane oxidation by sulphate during pauses in sedimentation  
1023 accords with the field and geochemical evidence for cementation close to the sediment-water  
1024 interface (Sections 6 and 7). However, although initiation of limestone formation started early,  
1025 final cementation appears to have occurred well below the sediment-water interface (Section  
1026 7). Such a history explains the overall rarity of limestone intraclasts despite the prevalence of  
1027 sea-floor erosion and re-deposition of sediments in storm events.

1028 The restriction of protrusive *Diplocraterion* traces to light marls and limestone beds  
1029 supports the idea that deposition of light marl, rather than dark marl or black laminated-shale,  
1030 was often associated with significant bottom-water turbulence. At Lyme Regis, increased  
1031 proportions of angular- compared to rounded-wood particles, interpreted as indicating  
1032 relatively high bottom-water turbulence, occur near the tops of many limestone beds and light  
1033 marls (Waterhouse, 1999a). This observation has apparently not been tested for the West  
1034 Somerset Coast (e.g. Bonis, Ruhl & Kürschner, 2010) probably because woody material is  
1035 much rarer.

1036 The explanation of orbital-climatic (Milankovitch) control of the alternations of  
1037 homogenized organic-carbon poor sediments with laminated organic carbon-rich sediments in  
1038 the offshore facies of the Blue Lias and correlatives remains popular (House, 1985; 1986;  
1039 Weedon, 1986; 1987a; 1987b, Waterhouse 1999a; 1999b; Weedon *et al.*, 1999; Hanzo *et al.*,

1040 2000; Bonis, Ruhl & Kürschner, 2010; Ruhl *et al.*, 2010). Intervals of increased fluvial drainage  
1041 during wetter climates are likely to have led to salinity stratification, enhanced stability of the  
1042 water column and increased fluxes of clay minerals from land. These factors were probably  
1043 significant in promoting both higher productivity and preservation of marine organic matter in  
1044 the darker laminated and more clay-rich sediments (Weedon, 1986; Fleet *et al.*, 1987).

1045         The precursors to the limestone beds, the light marls, were probably not only associated  
1046 with a relatively dry climate compared to the dark marl and black laminated shale deposition  
1047 (Weedon, 1986), but also stormier conditions (Waterhouse, 1999b). The increased storminess  
1048 causing erosion and/or winnowing during the deposition of light marl would have frequently  
1049 led to pauses in sedimentation (non-deposition and/or hiatuses) so that limestone beds could be  
1050 formed. However, increases in water depth and accommodation space, such as during the  
1051 Liasicus Zone, would have reduced the probability that storms would promote the formation  
1052 of limestones during deposition of light marl.

1053         The palaeo-latitude of southern Britain was about 35° N in the Early Jurassic (Smith,  
1054 Smith & Funnell, 1994). The ‘stormier’ climate associated with deposition of light marl is  
1055 envisaged as resulting from rare intense tropical cyclones, rather from than frequent mid-  
1056 latitude depressions. Increased storm influence during deposition of light marl (more frequent  
1057 turbulent bottom water) is consistent with a drier climate overall (less rainfall and lower flux  
1058 of clay). Such storm events led to episodic increases in bottom-water turbulence well below  
1059 the normal storm wave-base. Individual storm events could have led to sea-floor erosion, but  
1060 multiple storms would have been necessary for the prolonged phases of non-deposition  
1061 required for the initiation of limestone formation by carbonate cementation of light marls near  
1062 the sediment-water interface.

1063         In the Blue Lias Formation as a whole, beds of dark grey to black laminated limestone  
1064 and layers of laminated limestone nodules are much rarer than the homogeneous limestones.

1065 This distribution of lithologies was apparently because, at the associated water depths and in  
1066 the wetter climatic regime associated with the laminated shales (with high clay fluxes), storms  
1067 were usually too rare and/or too weak to cause pauses in sedimentation. In the field, laminated  
1068 limestone nodules at Lavernock and Southam Quarry show thicker laminae in the centres of  
1069 nodules that pinch laterally into much thinner laminae within the enclosing laminated shales  
1070 (Weedon, 1987a). Hence, laminated limestones apparently formed prior to significant  
1071 compaction just like the homogeneous grey limestone beds (Weedon, 1986; 1987a; Arzani,  
1072 2004). However, exceptionally ‘clean’ laminated limestone beds such as bed H30 (Intruder) at  
1073 Lyme Regis may represent deposition from low-density turbidity currents (Hesselbo &  
1074 Jenkyns, 1995).

1075         The observations of gutter casts and crustacean escape structures in Southam Quarry at  
1076 Long Itchington prove that storms manifestly caused sea-floor erosion and re-deposition during  
1077 times of laminated-shale deposition (Radley, 2008; O’Brien, Braddy & Radley, 2009). In  
1078 general, laminated limestones are most abundant within the Tilmanni and Planorbis zones.  
1079 Hence during the early Hettangian, water depths were apparently shallow enough for even  
1080 rare/weak storms to cause the pauses in sedimentation required to generate laminated limestone  
1081 beds and laminated limestone nodule layers.

1082         According to the Raiswell (1988) model of anaerobic methane oxidation by sulphate,  
1083 limestone formation started a metre so below the sediment-water interface. The range of  
1084 preservation of ammonites (Section 6) indicates that for different limestone beds the  
1085 cementation formed a framework-supporting fabric: a) before aragonite dissolution and before  
1086 compaction (ammonites fully preserved), b) after aragonite dissolution, but before significant  
1087 compaction (only external moulds of sediment-free inner whorls preserved, especially on the  
1088 edges of limestone beds) and c) after aragonite dissolution and after compaction started (no  
1089 ammonites shells preserved, although calcitic oyster xenomorphs may be present).

1090 Paul, Allison & Brett (2008) argued that the ammonites within the limestones at Lyme  
1091 Regis were preserved due to rapid deposition, which seems plausible, given the evidence for  
1092 storm-related deposition (Section 5, Weedon, 1986; 1987a; Waterhouse, 1999b; Radley, 2008).  
1093 However, not mentioned by Paul, Allison & Brett (2008), was that additionally an interval of  
1094 non-deposition after the rapid burial by light marl seems also to have been necessary to initiate  
1095 limestone formation. Given the homogenization of the light marl by burrowers prior to  
1096 limestone formation, the non-deposition and cementation apparently did not immediately  
1097 follow rapid sedimentation. However, unless non-deposition occurred before aragonite  
1098 dissolution (i.e. within a few thousand years), cementation would not have been early enough  
1099 to preserve the ammonites.

1100 The Blue Lias Formation is well known for fully articulated ichthyosaur and plesiosaur  
1101 fossils (e.g. Milner & Walsh, 2010). Skeletons enclosed by laminated shale were probably  
1102 protected from scavengers by bottom-water anoxia. However, given that many fully articulated  
1103 skeletons that somehow avoided disarticulation by scavengers are found also in the marls and  
1104 homogeneous limestones, rapid burial of carcasses during storms could also explain their  
1105 preservation.

1106 Normally, the aragonite of ammonites buried within accumulating light marl would  
1107 have dissolved and left no trace unless pyritized (very rare in the Blue Lias Formation) or  
1108 preserved as external moulds in oyster xenomorphs. Limestone beds that do not preserve  
1109 ammonites were apparently formed during phases of non-deposition that did not quickly follow  
1110 an episode of rapid light marl deposition.

1111

## 1112 **9. Conclusions**

1113 In the offshore hemipelagic facies of the Blue Lias Formation, the spacing of individual  
1114 limestones within zones and the varying limestone proportions of limestones from zone-to-

1115 zone and from site-to-site, can all be related to the bottom-water turbulence. The model adopted  
1116 represents a synthesis of several key papers accompanied by the new biostratigraphic and  
1117 sedimentological data presented here.

1118         There is abundant evidence for winnowing, non-deposition and sea-floor erosion within  
1119 the formation, as indicated by the Shaw plot (Fig. 8) and the field evidence (Section 5).  
1120 Initiation of limestone formation is explained by periods of non-deposition causing  
1121 cementation of the zone of anaerobic methane oxidation by sulphate close to the sediment-  
1122 water interface (Raiswell, 1988, Bottrell & Raiswell, 1989). This mechanism explains the  
1123 decoupling of limestone bed thickness from lateral and stratigraphic variations in net  
1124 accumulation rate (Hallam, 1964; Raiswell, 1988). The periods of increased sea-floor erosion  
1125 or non-deposition that initiated the formation of individual limestone beds and horizons of  
1126 limestone nodules can be attributed to storms (Weedon, 1986; 1987a; Waterhouse 1999b;  
1127 Radley, 2008).

1128         Deposition of light marl was associated with a drier climate characterized by much  
1129 stronger and/or more frequent, though possibly still rare, major storms whereas more tranquil  
1130 conditions were typical for the deposition of dark marl and laminated shale (Waterhouse,  
1131 1999b). Thus, limestone beds and nodule horizons were much more likely to form within light  
1132 marl beds. However, occasionally during deposition of laminated shale, storms did lead to non-  
1133 deposition and formation of laminated limestone beds and laminated limestone nodule horizons  
1134 (Radley, 2008). Relatively shallow water depths during the Tilmanni and Planorbis Zones, and  
1135 thus greater influence of storms on bottom-water turbulence during laminated-shale deposition,  
1136 explains the concentration of laminated limestones within this interval. Conversely, relatively  
1137 greater water depths, for example during the Liasicus Zone, meant that storm-related bottom-  
1138 water turbulence was reduced and thus less likely to cause non-deposition and the formation  
1139 of homogeneous limestone beds and nodule horizons within the light marls.

1140           A strong storm influence on deposition in the offshore Blue Lias Formation is not  
1141 surprising, given the well-known storm-related deposition of the ‘marginal facies’ (Johnson &  
1142 McKerrow, 1995; Simms, 2004; Sheppard, 2006) and of the near-shore facies of the Blue Lias  
1143 in South Wales (Section 4.a, Sheppard, Houghton & Swan, 2006). Storm influences have also  
1144 been documented from Hettangian and Lower Sinemurian strata, of Blue Lias character, in the  
1145 Paris Basin (Hanzo *et al.*, 2000).

1146           In the Lower Pliensbachian of Yorkshire, Van Buchem, McCave & Weedon (1994)  
1147 showed that the orbitally forced cycles of grain size were related to varying storm intensity.  
1148 The coeval Belemnite Marls of Dorset (or Stonebarrow Marl Member of the Charmouth  
1149 Mudstone Formation of Page, 2010b) exhibit orbitally controlled alternations of light and dark  
1150 marls (Weedon & Jenkyns, 1999). Similar orbitally controlled cyclicity has been documented  
1151 in the Pliensbachian strata of the Mochras borehole at Llanbedr, Wales (Ruhl *et al.*, 2016).  
1152 Sellwood (1970) believed the rhythms of the Belemnite Marls indicated cycles in bottom-water  
1153 turbulence but invoked short-term changes in sea level as a primary forcing mechanism.  
1154 However, similarly to the Blue Lias, the changes in sediment composition in the Belemnite  
1155 Marls can be linked to orbital climatic cycles (Weedon & Jenkyns, 1999), with indications of  
1156 varying bottom-water turbulence (variations in characteristics of and types of burrow traces,  
1157 Sellwood, 1970) linked to cycles in storminess. Deeper water conditions compared to the  
1158 depositional environment of the Blue Lias may explain the lack of non-sequences and  
1159 consequent lack of limestones except at the base and top of the Belemnite Marls (Hesselbo &  
1160 Jenkyns, 1995; Weedon & Jenkyns, 1999).

1161           Normally, ammonites in the Blue Lias are not preserved in the light marls unless  
1162 represented by crushed specimens, commonly with associated organic films; or their former  
1163 presence may be indicated by oyster xenomorphs. Ammonites preserved within limestone beds  
1164 required rapid burial under light marl (Paul, Allison & Brett, 2008), most likely caused by



1165 storm-related re-deposition (Section 5, Radley, 2008). However, preservation would only  
1166 normally occur when rapid burial was followed fairly quickly by a period of non-deposition  
1167 that initiated limestone formation. Non-deposition was probably also linked to storm activity  
1168 and occurred after homogenization of the sediment by burrowers, but before aragonite  
1169 dissolution. If non-deposition or hiatus formation did not quickly follow rapid deposition,  
1170 formation of limestone beds devoid of ammonites took place, as a combination of aragonite  
1171 dissolution, bioturbation and early compaction removed all trace of the shells. Ammonites  
1172 within the laminated shales on the west coast of Somerset are preserved as: a) shell-less  
1173 impressions, b) impressions with residual brown films, c) as white aragonite, d) brown calcite  
1174 near faults or e) as pristine (i.e. iridescent) aragonite that is likely to have owed its survival to  
1175 the protective effects of organic matter.

1176         To account for the stable-isotope signatures of the limestone beds, it is suggested that  
1177 initially early carbonate cementation produced framework-supporting fabrics that were usually  
1178 strong enough to resist compaction of large macrofossils such as ammonites (if not previously  
1179 dissolved). However, the final oxygen- and carbon-isotope signatures within the limestones  
1180 represent a mixture of the early plus much later cement that filled the micrograde framework  
1181 pores. At Lyme Regis, due to the low net accumulation rate and the relatively shallow depths  
1182 at which cementation finished, the oxygen isotopes in the limestone beds are heavier than those  
1183 of marls and shales. By contrast, on the West Somerset coast, the much higher net accumulation  
1184 rates ensured that final cementation of the limestone beds occurred much deeper in the  
1185 sediment pile so that the overall oxygen-isotope values are generally lighter than the associated  
1186 marls and shales and also lighter than the limestones at Lyme Regis.

1187

### 1188         **Acknowledgements**

1189         The Royal Society provided a grant to G.P.W. in the early 1990s for the purchase of a

1190 Bartington MS meter. Stuart Robinson kindly supplied 38 ‘SAB’ samples (Hesselbo, Robinson  
1191 & Surlyk, 2004) from the Tilmanni and Planorbis biozones from St Audries Bay for MS  
1192 analysis to supplement the collection obtained by Weedon (1987a). Simon Robinson provided  
1193 helpful advice on interpretations of MS. Our thanks go to Chris Paul for his constructive  
1194 review.

1195 K.N.P. thanks the Orchard-Wyndham estate, including the late Dr Catherine Wyndham,  
1196 and the East Quantoxhead Estate, including the late Colonel Sir Walter Luttrell, for ongoing  
1197 permission to sample on the Estate’s foreshore areas in West Somerset. Bob Cornes and Tom  
1198 Sunderland of Natural England provided help and advice regarding permission for sampling in  
1199 West Somerset and within the Axmouth-Lyme Regis National Nature Reserve, west of Lyme  
1200 Regis, respectively. Raymond Roberts of Natural Resources Wales (formerly Countryside  
1201 Council for Wales) advised on the St. Mary’s Well Bay section at Lavernock. K.N.P. would  
1202 also like to thank María-José Bello-Villalba and Joseph Bello-Page for assistance in the field.

1203

## 1204 **References**

1205 Ager, D. 1986. A reinterpretation of the basal ‘Littoral Lias’ of the Vale of Glamorgan.  
1206 *Proceedings of the Geologists’ Association* **97**, 29–35.

1207 Allison, P. A., Hesselbo, S. P., & Brett, C. A. 2008. Methane seeps on an Early Jurassic  
1208 seafloor. *Palaeogeography, Palaeoclimatology, Palaeoecology* **270**, 230–238.

1209 Ambrose, K. 2001. The lithostratigraphy of the Blue Lias Formation (Late Rhaetian-Early  
1210 Sinemurian) in the southern part of the English Midlands. *Proceedings of the*  
1211 *Geologists’ Association* **112**, 97–110.

1212 Arzani, N. 2004. Diagenetic evolution of mudstones: black shales to laminated limestones, an  
1213 example from the Lower Jurassic of SW Britain. *Journal of Sciences Islamic Republic*  
1214 *of Iran* **15**, 257–267.

- 1215 Arzani, N. 2006. Primary versus diagenetic bedding in the limestone-marl/shale alternations of  
1216 the epeiric seas, an example from the Lower Lias (Early Jurassic) of SW Britain.  
1217 *Carbonates and Evaporites* **21**, 94–109.
- 1218 Barras, C. G. & Twitchett, R. J., 2007. Response of the marine infauna to Triassic-Jurassic  
1219 environmental change: ichnological data from southern England. *Palaeogeography,*  
1220 *Palaeoclimatology, Palaeoecology* **244**, 223–241.
- 1221 Bixler, W. G., Elmore, R. D., & Engel, M. H. 1998. The origin of magnetization and  
1222 geochemical alteration in a fault zone, Kilve, England. *Geological Journal* **33**, 89–105.
- 1223 Bleil, S. & Petersen, N. 1987. Magnetic properties of natural minerals. In *Physical properties*  
1224 *of rocks Volume 1 subvolume B* (ed G. Angenheister) pp. 308–365. Springer.
- 1225 Bloos, G. & Page, K. N. 2000a. The basal Jurassic ammonite succession in the North-West  
1226 European Province - Review and new results. In: *Advances in Jurassic Research 2000.*  
1227 *Proceedings of the Fifth International Symposium on the Jurassic System* (eds R. L.  
1228 Hall & P. Smith), pp. 27–40. GeoResearch Forum **6**, Trans Tech Publications.
- 1229 Bloos, G. & Page, K. N. 2000b. The proposed GSSP for the base of the Sinemurian Stage near  
1230 East Quantoxhead/West Somerset (SW England) - The ammonite sequence. In:  
1231 *Advances in Jurassic Research 2000. Proceedings of the Fifth International Symposium*  
1232 *on the Jurassic System* (eds R. L. Hall & P. L. Smith) pp. 13–26. GeoResearch Forum  
1233 **6**, Trans Tech Publications.
- 1234 Bloos, G. & Page, K. N. 2002. The Global Stratotype Section and Point for base of the  
1235 Sinemurian Stage (lower Jurassic). *Episodes* **25**, 22–28.
- 1236 Bonis, N. A., Ruhl, M. & Kürschner, W.M. 2010. Milankovitch-scale palynological turnover  
1237 across the Triassic–Jurassic transition at St. Audrie’s Bay, SW UK. *Journal of the*  
1238 *Geological Society, London* **167**, 877–888.

- 1239 Bottrell, S. & Raiswell, R. 1989. Primary versus diagenetic origin of Blue Lias rhythms  
1240 (Dorset, UK): evidence from sulphur geochemistry. *Terra Nova* **1**, 457–456.
- 1241 Bown, P.R. 1987. Taxonomy, evolution, and biostratigraphy of late Triassic-early Jurassic  
1242 calcareous nannofossils. *Special Papers in Palaeontology* **38**, Palaeontological  
1243 Association, 118 pp.
- 1244 Bown, P. R. & Cooper, M. K. E. 1998. Jurassic. In *Calcareous Nannofossil Biostratigraphy*,  
1245 (ed. P. R. Bown), pp. 34–85. British Micropalaeontological Society Publications Series,  
1246 Chapman and Hall.
- 1247 Bromley, R. G. & Ekdale, A. A. 1984. *Chondrites*: a trace fossil indicator of anoxia in  
1248 sediments. *Science* **224**, 872–874.
- 1249 Bukri, P. M., Dent Glasser, L. S. & Smith, D. N. 1982. Surface coatings on ancient coccoliths.  
1250 *Nature* **297**, 145–147.
- 1251 Callomon, J. 1985. Biostratigraphy, chronostratigraphy and all that - again! In: *International*  
1252 *Symposium on Jurassic Stratigraphy, Erlangen 1984* (eds O. Michelsen, O. & A. A.  
1253 Zeiss), pp. 611-624. Geological Survey of Denmark, Copenhagen 3.
- 1254 Callomon, J. 1995. Time from fossils: S.S. Buckman and Jurassic high-resolution  
1255 geochronology. *Milestones in Geology* (ed. M. L. Le Bas), pp. 127–150. Geological  
1256 Society Memoir 16.
- 1257 Campos, J. G. & Hallam, A. 1979. Diagenesis of English Lower Jurassic limestones as inferred  
1258 from oxygen and carbon isotope analysis. *Earth and Planetary Science Letters* **45**, 23–  
1259 31.
- 1260 Clémence, M-E., Bartolini, A., Gardin, S., Paris, G., Beaumont, V. & Page, K. N. 2010. Early  
1261 Hettangian benthic-planktonic coupling at Doniford (SW England).  
1262 Palaeoenvironmental implications from the aftermath of the end-Triassic crisis.  
1263 *Palaeogeography, Palaeoclimatology, Paleoecology* **295**, 102–115.

- 1264 Clements, R. G. & members of the field studies in local geology class 1975. *The geology of the*  
1265 *Long Itchington Quarry (Rugby Portland Cement Co. Ltd., Southam Works)*. Percival  
1266 Guildhall, Rugby and Dept. of Geology, University of Leicester, 30 pp.
- 1267 Clements, R. G. & members of the field studies in local geology class, Percival Guildhouse,  
1268 Rugby 1977. *The Geology of the Parkfield Quarry, Rugby (Rugby Portland Cement Co.*  
1269 *Ltd., Rugby Works, Rugby, Warwickshire)*. Dept. of Geology, University of Leicester,  
1270 54 pp.
- 1271 Collinson, D. W., 1983. *Methods in rock magnetism and palaeomagnetism: Techniques and*  
1272 *Instrumentation*. Chapman and Hall, London, 503 pp.
- 1273 Cornford, C. 2003. Triassic palaeopressure and Liassic mud volcanoes near Kilve, west  
1274 Somerset. *Geoscience in South-West England* **10**, 430–434.
- 1275 Curtis, C. D., Cope, J. C. W., Plant, D. & Macquaker, J. H. S. 2000. ‘Instantaneous’  
1276 sedimentation, early microbial sediment strengthening and a lengthy record of chemical  
1277 diagenesis preserved in Lower Jurassic ammonitiferous concretions from Dorset.  
1278 *Journal of the Geological Society, London* **157**, 165–177.
- 1279 Day, E. C. H. 1865. On the Lower Lias of Lyme Regis. *Geological Magazine* **2**, 518–519.
- 1280 Deconinck, J-F., Hesselbo, S. P., Debuisser, N., Averbuch, O., Baudin, F. and Bessa, J. 2003.  
1281 Environmental controls on clay mineralogy of an Early Jurassic mudrock (Blue Lias  
1282 Formation, southern England). *International Journal of Earth Sciences* **92**, 255–266.
- 1283 Donovan, D. T. 1956. The zonal stratigraphy of the Blue Lias around Keynsham, Somerset.  
1284 *Proceedings of the Geologists’ Association* **66**, 182–212.
- 1285 Donovan, D. T., Horton, A., & Ivimey-Cook, H. C. 1979. The transgression of the Lower Lias  
1286 over the northern flank of the London Platform. *Journal of the Geological Society,*  
1287 *London* **136**, 165–173.

- 1288 Donovan, D. T. & Kellaway, G. A. 1984. *Geology of the Bristol District; the Lower Jurassic*  
1289 *rocks*. Memoir of the British Geological Survey Special Sheet. HMSO, 69 pp.
- 1290 Fleet, A. J., Clayton, C. J., Jenkyns, H. C. & Parkinson, D. N. (1987). Liassic source rock  
1291 deposition in western Europe (eds J. Brooks & K. Glennie) pp 59–70. In *Petroleum*  
1292 *Geology of north-west Europe, 1*, Graham & Trotman, London.
- 1293 Fletcher, C. J. N. 1988. Tidal erosion, solution cavities and exhalative mineralization associated  
1294 with the Jurassic unconformity at Ogmore, South Glamorgan. *Proceedings of the*  
1295 *Geologists' Association* **99**, 1–14.
- 1296 Gallois, R. W. & Paul, C. R. C. 2009. Lateral variations in the topmost part of the Blue Lias  
1297 and basal Charmouth Mudstone Formations (Lower Jurassic) on the Devon and Dorset  
1298 Coast. *Geoscience in South-West England* **12**, 125–133.
- 1299 Gluyas, J. G. 1984. Early carbonate diagenesis within Phanerozoic shales and sandstones of  
1300 the NW European shelf. *Clay Minerals* **19**, 309–321.
- 1301 Hall, A. & Kennedy, W. J. 1967. Aragonite in fossils. *Philosophical Transactions of the Royal*  
1302 *Society, London* **B168**, 377–412.
- 1303 Hallam, A. 1960. A sedimentary and faunal study of the Blue Lias of Dorset and Glamorgan.  
1304 *Philosophical Transactions of the Royal Society, London* **B243**, 1–44.
- 1305 Hallam, A. 1964. Origin of limestone-shale rhythms in the Blue Lias of England: a composite  
1306 theory. *Journal of Geology* **72**, 157–169.
- 1307 Hallam, A. 1981. A revised sea-level curve for the early Jurassic. *Journal of the Geological*  
1308 *Society, London* **138**, 735–743.
- 1309 Hallam, A., 1986. Origin of minor limestone-shale cycles: climatically induced or diagenetic?  
1310 *Geology* **14**, 609–612.
- 1311 Hallam, A., 1987. Reply to Weedon, 1987 Comment on: 'Origin of limestone-shale cycles:  
1312 climatically induced or diagenetic?' *Geology* **15**, 93–94.

- 1313 Hallam, A. 1997. Estimates of the amount and rate of sea-level change across the Rhaetian–  
1314 Hettangian and Pliensbachian–Toarcian boundaries (latest Triassic to early Jurassic).  
1315 *Journal of the Geological Society, London* **154**, 773–779.
- 1316 Hallam, A. & Bradshaw, M. J. 1979. Bituminous shales and oolitic ironstones as indicators of  
1317 transgression and regression. *Journal of the Geological Society, London* **136**, 157–164.
- 1318 Hamilton, G. B. 1982. Triassic and Jurassic calcareous nannofossils. In *A stratigraphical index*  
1319 *of calcareous nannofossils* (ed. A. R. Lord), pp. 17–39. British Micropalaeontological  
1320 Society Series, Ellis Horwood, Chichester.
- 1321 Hanzo, M., Lathuilière, B., Alméras, Y., Dagallier, G., Guérin-Franiatte, S., Guillocheau, F.,  
1322 Huault, V., Nori, L. & Rauscher, R. 2000. Paléoenvironnements dans le Calcaire à  
1323 gryphées du Lias de Lorraine, de la carrière de Xeulley au Bassin parisien. *Eclogae*  
1324 *Geologicae Helveticae* **93**, 183–206.
- 1325 Hays, J. D., Imbrie, J. & Shackleton, N. J. 1976. Variations in the Earth’s orbit: pacemaker of  
1326 the ice ages. *Science* **194**, 1121–1132.
- 1327 Hesselbo, S. P. 2008. Sequence stratigraphy and inferred relative sea-level change from the  
1328 onshore British Jurassic. *Proceedings of the Geologists’ Association* **119**, 19–34.
- 1329 Hesselbo, S. P. & Jenkyns, H. C. 1995. A comparison of the Hettangian to Bajocian successions  
1330 of Dorset and Yorkshire. In *Field Geology of the British Jurassic* (ed P. D. Taylor) pp.  
1331 105–150. Geological Society, London.
- 1332 Hesselbo, S. P. & Jenkyns, H. C. 1998. British Lower Jurassic sequence stratigraphy. In  
1333 *Mesozoic and Cenozoic Sequence Stratigraphy of European Basins* (eds J. Hardenbol,  
1334 J. Thierry, M. B. Farley, T. Jacquin, P-C. de Graciansky & P. Vail) pp. 562–581. SEPM  
1335 Special Publication 60.

- 1336 Hesselbo, S. P., Robinson, S. A. & Surlyk, F. 2004. Sea-level change and facies development  
1337 across potential Triassic-Jurassic boundary horizons, SW Britain. *Journal of the*  
1338 *Geological Society, London* **161**, 365–379.
- 1339 Hillebrandt, A. V., Krystyn, L., & Kuerschner, W. M. 2007. A candidate GSSP for the base of  
1340 the Jurassic in the Northern Calcareous Alps (Kuhjoch section, Karwendel Mountains,  
1341 Tyrol, Austria). *International Sub-commission on Jurassic Stratigraphy Newsletter* **34**,  
1342 2–20.
- 1343 Hillebrandt, A. V. & Krystyn, L. 2009. On the oldest Jurassic ammonites of Europe (Northern  
1344 Calcareous Alps, Austria) and their global significance. *Neues Jahrbuch für Geologie*  
1345 *und Paläontologie, Abhandlungen* **253**, 163–195.
- 1346 Hodges, P. 1986. The Lower Lias (Lower Jurassic) of the Bridgend area, South Wales.  
1347 *Proceedings of the Geologists' Association* **97**, 237–242.
- 1348 Hodges, P. 1994. The base of the Jurassic System: new data on the first appearance of  
1349 *Psiloceras planorbis* in southwest Britain. *Geological Magazine* **131**, 841–844.
- 1350 Hounslow, M. W. 1985. Magnetic fabric arising from paramagnetic phyllosilicate minerals in  
1351 mudrocks. *Journal of the Geological Society, London* **142**, 995–1106.
- 1352 Hounslow, M. W., Posen, P. E. & Warrington, G. 2004. Magnetostratigraphy and  
1353 biostratigraphy of the Upper Triassic and lowermost Jurassic succession, St. Audrie's  
1354 Bay, UK. *Palaeogeography, Palaeoclimatology, Palaeoecology* **213**, 331–358.
- 1355 House M. R. 1985. A new approach to an absolute time scale from measurements of orbital  
1356 cycles and sedimentary microrhythms. *Nature* **313**, 17–22.
- 1357 House, M. R. 1986. Are Jurassic microrhythms due to orbital forcing? *Proceedings of the*  
1358 *Ussher Society* **6**, 299–311.
- 1359 Hudson, J. D. & Martill, D. M. 1991. The Lower Oxford Clay: production and preservation of  
1360 organic matter in the Callovian (Jurassic) of central England. In *Modern and ancient*



- 1361 *continental Shelf Anoxia* (eds R. V. Tyson & T. H. Pearson), pp. 363–379. Geological  
1362 Society, London Special Publication 58.
- 1363 Jenkyns, H. C., Jones, C. E., Gröcke, D. R., Hesselbo, S. P. & Parkinson, D. N. 2002.  
1364 Chemostratigraphy of the Jurassic System: applications, limitations and implications  
1365 for palaeoceanography. *Journal of the Geological Society, London* **159**, 351–378.
- 1366 Jenkyns, H. C. & Senior, J. R. 1991. Geological evidence for intra-Jurassic faulting in the  
1367 Wessex Basin and its margins. *Journal of the Geological Society, London* **148**, 245–  
1368 260.
- 1369 Johnson, M. E. & McKerrow, W. S. 1995. The Sutton Stone: an early Jurassic rocky shoreline  
1370 deposit in South Wales. *Palaeontology* **38**, 529–541.
- 1371 Kent, P. E. 1936. The formation of hydraulic limestones of the Lower Lias. *Geological*  
1372 *Magazine* **73**, 476–478.
- 1373 Kent, P. E. 1937. The Lower Lias of South Nottinghamshire. *Proceedings of the Geologist's*  
1374 *Association* **48**, 163–174.
- 1375 Korte, C., Hesselbo, S. P., Jenkyns, H. C., Rickaby, R. E., & Spotl, C. 2009.  
1376 Palaeoenvironmental significance of carbon- and oxygen-isotope stratigraphy of  
1377 marine Triassic–Jurassic boundary sections in SW Britain. *Journal of the Geological*  
1378 *Society, London* **166**, 432–445.
- 1379 Lang, W. D. 1924. The Blue Lias of the Devon and Dorset Coasts. *Proceedings of the*  
1380 *Geologists' Association* **35**, 169–184.
- 1381 Lees, J. A., Bown, P. R. & Young, J. R. 2006. Photic zone palaeoenvironments of the  
1382 Kimmeridge Clay Formation (Upper Jurassic, UK) suggested by calcareous  
1383 nannoplankton palaeoecology. *Palaeogeography, Palaeoclimatology, Palaeoecology*  
1384 **235**, 110–134.

- 1385 Loughman, D. L. 1982. *A facies analysis of the Triassic/Jurassic boundary beds of the world:*  
1386 *with special reference to North-West Europe and the Americas.* Ph.D. Thesis University  
1387 of Birmingham (unpublished).
- 1388 Marshall, J. D. 1982. Isotopic composition of displacive fibrous calcite veins: reversals in pore-  
1389 water composition trends during burial diagenesis. *Journal of Sedimentary Petrology*  
1390 **52**, 615–630.
- 1391 Milner, A.C. and Walsh, S., 2010. Reptiles. In *Fossils from the Lower Lias of the Dorset Coast*,  
1392 (eds A. R. Lord & P. G. Davis), pp. 372–394. Palaeontological Association, London.
- 1393 Moghadam, H. V. & Paul., C. R. C. 2000. Trace fossils of the Jurassic, Blue Lias, Lyme Regis,  
1394 Southern England. *Ichnos* **7**, 283–306.
- 1395 O'Brien, L. J., Braddy, S. J., & Radley, J. D. 2009. A new arthropod resting trace and associated  
1396 suite of trace fossils from the Lower Jurassic of Warwickshire, England. *Palaeontology*  
1397 **52**, 1099–1112.
- 1398 Odin, G. S. & Matter, A. 1981. De glauconiarum origine. *Sedimentology* **28**, 611-641.
- 1399 Ogg, J. G. & Hinnov, L. A. 2012. Jurassic. In *The Geologic Time Scale 2012* (eds F. M.  
1400 Gradstein, J. G. Ogg, M. Schmitz & G. Ogg), pp. 731–791. Elsevier.
- 1401 Old, R. A., Sumbler, M. G., & Ambrose. K. 1987. *Geology of the Country around Warwick.*  
1402 Memoir of the British Geological Survey Sheet 84 (England and Wales).
- 1403 Page, K. N. 1992. The sequence of ammonite-correlated horizons in the British Sinemurian  
1404 (Lower Jurassic). *Newsletters on Stratigraphy* **27**, 129–156.
- 1405 Page, K. N. 1995. East Quantoxhead, Somerset, England: a potential Global Stratigraphic  
1406 Section and Point (GSSP) for the base of the Sinemurian Stage (Lower Jurassic).  
1407 *Proceedings of the Ussher Society* **9**, 446–450.

- 1408 Page, K. N. 2002. A review of the ammonite faunas and standard zonation of the Hettangian  
1409 and Lower Sinemurian succession (Lower Jurassic) of the East Devon Coast (South  
1410 west England). *Geoscience in South-West England* **10**, 293–303.
- 1411 Page, K. N. 2003. The Lower Jurassic of Europe - its subdivision and correlation. In *The*  
1412 *Jurassic of Denmark and adjacent areas* (eds J. Ineson, & F. Surlyk), pp. 23–59.  
1413 Geological Survey of Denmark and Greenland, Bulletin 1.
- 1414 Page, K. N. 2005. The Hettangian ammonite faunas of the west Somerset Coast (South West  
1415 England) and their significance for the correlation of the candidate GSSP (Global  
1416 Stratotype and Point) for the base of the Jurassic System at St. Audries Bay. *Còlloque*  
1417 *l'Hettangien a Hettange de la science au patrimoine*, Université Henri Poincaré, pp.  
1418 15–19.
- 1419 Page, K. N. 2010a. High resolution ammonite stratigraphy of the Charmouth Mudstone  
1420 Formation (Lower Jurassic: Sinemurian-Lower Pliensbachian) in south-west England,  
1421 UK. *Volumina Jurassica* **7**, 19–29.
- 1422 Page, K. N. 2010b. Stratigraphical framework. In *Fossils from the Lower Lias of the Dorset*  
1423 *Coast* (eds A. R. Lord & P. G. Davis), pp. 33–53. Palaeontological Association Field  
1424 Guides to Fossils 13.
- 1425 Page, K. N. 2010c. Ammonites. In *Fossils from the Lower Lias of the Dorset Coast* (eds A. R.  
1426 Lord & P. G. Davis), pp. 169–261. Palaeontological Association Field Guides to Fossils  
1427 13.
- 1428 Page, K. N. in press. From Opper to Callomon (and beyond!): building a high resolution  
1429 ammonite-based biochronology for the Jurassic System. *Lethaia*.
- 1430 Page, K. N. & Bloos, G. 1995. The base of the Jurassic System in West Somerset, South-West  
1431 England – new observations on the succession of ammonite faunas of the lowermost  
1432 Hettangian Stage. *Geoscience in South-West England* **9**, 231–235.

- 1433 Page, K. N., Bloos, G., Bessa, J. L., Fitzpatrick, M., Hart, M. B., Hesselbo, S., Hylyon, M.,  
1434 Morris, A. & Randall, D. E. 2000. East Quantoxhead, Somerset: A candidate Global  
1435 Stratotype Section and Point for the base of the Sinemurian Stage (Lower Jurassic). In  
1436 *Advances in Jurassic Research 2000* (eds R. L. Hall & P. L. Smith), pp. 163–72. Proc.  
1437 Fifth International Symposium on the Jurassic System, GeoResearch Forum 6, Trans  
1438 Tech Publications.
- 1439 Palmer, C. P. 1972. The Lower Lias (Lower Jurassic) between Watchet and Lilstock in North  
1440 Somerset (United Kingdom). *Newsletters on Stratigraphy* **2**, 1–30.
- 1441 Paul, C. R. C., Allison, P.A. & Brett, C. E. 2008. The occurrence and preservation of ammonites  
1442 in the Blue Lias Formation (lower Jurassic) of Devon and Dorset, England and their  
1443 palaeoecological, sedimentological and diagenetic significance. *Palaeogeography,*  
1444 *Palaeoclimatology, Palaeoecology* **270**, 258–272.
- 1445 Paris, G., Beaumont, V., Bartolini, A., Clémence, M-E. & Gardin, S. 2010. Nitrogen isotope  
1446 record of a perturbed paleoecosystem in the aftermath of the end-Triassic crisis,  
1447 Doniford section, SW England. *Geochemistry, Geophysics, Geosystems* **11**, Q08021,  
1448 doi:10.1029/2010GC003161.
- 1449 Pearson, S. J., Marshall, J. E. A. & Kemp, A. E. S. 2004. The White Stone Band of the  
1450 Kimmeridge Clay Formation, an integrated high-resolution approach to understanding  
1451 environmental change. *Journal of the Geological Society, London* **161**, 675–683.
- 1452 Price, G. D., Vowles-Sheridan, N. & Anderson, M. W. 2008. Lower Jurassic mud volcanoes  
1453 and methane, Kilve, Somerset, UK. *Proceedings of the Geologists' Association* **119**,  
1454 193–201.
- 1455 Radley, J. D. 2008. Seafloor erosion and sea-level: Early Jurassic Blue Lias Formation of  
1456 central England. *Palaeogeography, Palaeoclimatology, Palaeoecology* **270**, 287–294.

- 1457 Raiswell, R. 1988. Chemical model for the origin of minor limestone-shale cycles by anaerobic  
1458 methane oxidation. *Geology* **16**, 641–644.
- 1459 Raiswell, R. & Fisher, Q. J. 2000. Mudrock-hosted carbonate concretions: a review of growth  
1460 mechanisms and their influence on chemical and isotopic composition. *Journal of the*  
1461 *Geological Society, London* **157**, 239–251.
- 1462 Richardson, L. 1905. The Rhaetic and contiguous deposits of Glamorganshire. *Quarterly*  
1463 *Journal of the Geological Society, London* **61**, 385–424.
- 1464 Richardson, W. A. 1923. Petrology of the Shales-with-‘Beef’. *Quarterly Journal of the*  
1465 *Geological Society, London* **79**, 88–98.
- 1466 Ruhl, M., Deenen, M. H. L., Abels, H. A., Bonis, N. R., Krijgsman, W. & Kürschner, W. M.  
1467 2010. Astronomical constraints on the duration of the early Jurassic Hettangian stage  
1468 and recovery rates following the end-Triassic mass extinction (St. Audrie’s Bay/East  
1469 Quantoxhead, UK). *Earth and Planetary Science Letters* **296**, 262–276.
- 1470 Ruhl, M., Hesselbo, S. P., Hinnov, L., Jenkyns, H. C., Xu, W., Riding, J. B., Storm, M.,  
1471 Minisini, D., Ullmann, C. V. & Leng, M. J. 2016. Astronomical constraints on the  
1472 duration of the Early Jurassic Pliensbachian Stage and global climatic fluctuations.  
1473 *Earth and Planetary Science Letters* **455**, 149–165.
- 1474 Seilacher, A. 2007. *Trace Fossil Analysis*. Springer, 226 pp.
- 1475 Sellwood, B. W. 1970. The relation of trace fossils to small-scale sedimentary cycles in the  
1476 British Lias. In *Trace Fossils* (eds T. R. Crimes & J. C. Harper), pp. 489–504.  
1477 *Geological Journal Special Issue 3*.
- 1478 Sellwood, B. W. & Jenkyns, H. C. 1975. Basins and swells and the evolution of an epeiric sea  
1479 (Pliensbachian–Bajocian of Great Britain). *Journal of the Geological Society, London*  
1480 **131**, 373–388.

- 1481 Sheppard, H. T. 2006. Sequence architecture of ancient rocky shorelines and their response to  
1482 sea-level change: an Early Jurassic example from South Wales, UK. *Journal of the*  
1483 *Geological Society, London* **163**, 595–606.
- 1484 Sheppard, H. T., Houghton, R. D. & Swan, A. R. H. 2006. Bedding and pseudo-bedding in the  
1485 Early Jurassic of Glamorgan: deposition and diagenesis of the Blue Lias in South  
1486 Wales. *Proceedings of the Geologists' Association* 117, 249–264.
- 1487 Shukri, N. M. 1942. Rhythmic bedding in the Lower Lias of England. *Faculty of Science Fouad*  
1488 *I University Cairo Bulletin* **24**, 66–73.
- 1489 Simms, M. J. 2004. British Lower Jurassic Stratigraphy: an Introduction. In *British Lower*  
1490 *Jurassic Stratigraphy* (eds M. J. Simms, N. Chidlaw, N. Morton, & Page, K. N.) pp. 3–  
1491 51. Geological Conservation Review Series 30.
- 1492 Simms, M. J., Little, C. T. S. & Rosen, B. R. 2002. Corals not serpulids: mineralized colonial  
1493 fossils in the Lower Jurassic marginal facies of South Wales. *Proceedings of the*  
1494 *Geologists' Association* **113**, 31–36.
- 1495 Smith, A. G. Smith, D. G. & Funnell, B. M. 1994. *Atlas of Mesozoic and Cenozoic Coastlines*.  
1496 Cambridge University Press, 99 pp.
- 1497 Smith, D. G. 1989. Stratigraphic correlation of presumed Milankovitch cycles in the Blue Lias  
1498 (Hettangian to earliest Sinemurian), England. *Terra Nova* **1**, 457–460.
- 1499 Trueman, A. E., 1920. The Liassic rocks of the Cardiff District. *Proceedings of the Geologists'*  
1500 *Association* **31**, 93–107.
- 1501 Trueman, A. E. 1922. The Liassic rocks of Glamorgan. *Proceedings of the Geologists'*  
1502 *Association* **33**, 245–284.
- 1503 Trueman, A. E. 1930. The Lower Lias (Bucklandi Zone) of Nash Point, Glamorgan.  
1504 *Proceedings of the Geologists' Association* **61**, 149–159.

- 1505 Van Buchem, F. S. P., McCave, I. N. & Weedon, G. P. 1994. Orbitally induced small-scale  
1506 cyclicity in a siliciclastic epicontinental setting (Lower Lias, Yorkshire, UK). In *Orbital*  
1507 *Forcing and Cyclic Sequences* (eds P.L. de Boer & D.G. Smith), pp. 345–366.  
1508 International Association of Sedimentologists Special Publication 19.
- 1509 van de Schootbrugge, B., Tremolada, F., Rosenthal, Y., Bailey, T. R., Feist-Burkhardt, S.,  
1510 Brinkhuis, H., Pross, J., Kent, D. V. & Falkowski, P.G. 2007. End-Triassic calcification  
1511 crisis and blooms of organic-walled ‘disaster species’. *Palaeogeography,*  
1512 *Palaeoclimatology, Palaeoecology* **244**, 126–141.
- 1513 Warrington, G. & Ivimey-Cook, H. C. 1995. The Late Triassic and Early Jurassic of coastal  
1514 sections in west Somerset and South and Mid-Glamorgan. In *Field Geology of the*  
1515 *British Jurassic* (ed P. D. Taylor) pp. 9–30. Geological Society, London.
- 1516 Waterhouse, H. K. 1999a. Orbital forcing of palynofacies in the Jurassic of France and the  
1517 United Kingdom. *Geology* **27**, 511–514.
- 1518 Waterhouse, H. K. 1999b. Regular terrestrially derived palynofacies cycles in irregular marine  
1519 sedimentary cycles, Lower Lias, Dorset, UK. *Journal of the Geological Society,*  
1520 *London* **156**, 1113–1124.
- 1521 Waters, R. A. & Lawrence, D. J. D. 1987. *Geology of the South Wales Coalfield, Part III, the*  
1522 *country around Cardiff*. Memoir 1:50,000 Geological sheet 263 (England and Wales),  
1523 HMSO.
- 1524 Weedon, G. P. 1985. Palaeoclimatic information from ancient pelagic and hemipelagic cyclic  
1525 sediments. *Terra Cognita* **5**, 110.
- 1526 Weedon, G. P. 1986. Hemipelagic shelf sedimentation and climatic cycles: the basal Jurassic  
1527 (Blue Lias) of South Britain. *Earth and Planetary Science Letters* **76**, 321–335.

- 1528 Weedon, G. P. 1987a. *Palaeoclimatic significance of open-marine cyclic sequences*. D. Phil.  
1529 Thesis University of Oxford, 2 volumes available at:  
1530 <http://ora.ox.ac.uk/objects/uuid:aa009e6b-d429-4340-b3c5-30f5227f0148>.
- 1531 Weedon, G. P. 1987b. Comment on: ‘Origin of limestone-shale cycles: climatically induced or  
1532 diagenetic?’ by Hallam, A., 1986. *Geology* **15**, 92–94.
- 1533 Weedon, G. P., & Jenkyns, H. C. 1999. Cyclostratigraphy and the Early Jurassic time scale:  
1534 data from the Belemnite Marls, Dorset, southern England. *Geological Society of  
1535 America Bulletin* **111**, 1823–1840.
- 1536 Weedon, G. P., Jenkyns, H. C., Coe, A. L. & Hesselbo, S. P. 1999. Astronomical calibration  
1537 of the Jurassic time-scale from cyclostratigraphy in British mudrock formations.  
1538 *Philosophical Transactions of the Royal Society, London* **357**, 1787–1813.
- 1539 Whittaker, A. & Green, G. W. 1983. Geology of the country around Weston-super-Mare.  
1540 Memoire 1:50,000 Geological sheet 279, New series with parts of sheets 263 and 295,  
1541 HMSO.
- 1542 Whittaker, A., Holliday, D. W. & Penn, I. E. 1985. *Geophysical logs in British Stratigraphy*.  
1543 Geological Society Special Report 18, Geological Society, London, 74 pp.
- 1544 Wignall, P. B. 2001. Sedimentology of the Triassic-Jurassic boundary beds in Pinhay Bay  
1545 (Devon, SW England). *Proceedings of the Geologists’ Association* **112**, 349–360.
- 1546 Williams, R. B. G. 1984. *Introduction to Statistics for Geographers and Earth Scientists*.  
1547 MacMillan, 349 pp.
- 1548 Wilson, D., Davies, J. R., Fletcher, C. J. N. & Smith, M. 1990. *Geology of the South Wales  
1549 Coalfield, Part VI, the country around Bridgend*. Memoir 1:50,000 Geological sheets  
1550 261 and 262 (England and Wales), HMSO.
- 1551 Wobber, F. J. 1963. A directional structure from the Lower Jurassic of Great Britain. *Journal  
1552 of Sedimentary Petrology* **34**, 692–693.



- 1553 Wobber, F. J. 1965. Sedimentology of the Lias (Lower Jurassic) of South Wales. *Journal of*  
1554 *Sedimentary Petrology* **35**, 683–703.
- 1555 Wobber, F. J. 1966. A study of the depositional area of the Glamorgan Lias. *Proceedings of*  
1556 *the Geologists' Association* **77**, 127–137.
- 1557 Wright, V. P., Cherns, L. & Hodges, P. 2003. Missing molluscs: field testing taphonomic loss  
1558 in the Mesozoic through large-scale aragonite dissolution. *Geology* **31**, 211–214.
- 1559 Young, J. R. & Bown, P. R. 1991. An ontogenetic sequence of coccoliths from the Late Jurassic  
1560 Kimmeridge Clay of England. *Palaeontology* **4**, 843–850.

1561

1562 **Figure captions**

1563 Figure 1.

1564 (a) Location of the sections illustrated in Figs 3–6.

1565 (b) Formation characteristics according to Hettangian ammonite zone and location. Data from  
1566 logs shown in Fig 3–6. The symbols in Fig. 1a indicate the localities. The percentage of  
1567 limestone refers to the thickness of limestone logged as limestone or laminated limestone beds,  
1568 or if more than 50% of a particular level, limestone or laminated limestone nodules. Ave. =  
1569 average, L/D = Light/Dark, Lam. = laminated.

1570 (c) Average rock-type composition at Lyme Regis and on the West Somerset coast (St Audries  
1571 Bay and Quantock's Head sections) in terms of weight per cent calcium carbonate (%CaCO<sub>3</sub>),  
1572 total organic carbon (TOC) and TOC re-expressed on a carbonate-free basis (TOCcf).  
1573 Horizontal bars denote 95% confidence intervals around the mean. Data and analytical methods  
1574 from Weedon (1987a): 90 samples from the Angulata and Bucklandi zones at Lyme Regis and  
1575 57 samples from the Tilmanni to Bucklandi zones on the West Somerset coast. These data are  
1576 supplemented using a further 38 SAB samples (Hesselbo *et al.*, 2008) from the Tilmanni and  
1577 Planorbis zones at St Audries Bay. Numbers of samples analyzed by rock-type for Lyme Regis

1578 vs West Somerset coast respectively are: limestone and limestone nodules 31 vs 17; light marl  
1579 23 vs 17; dark marl 20 vs 19; laminated shale 16 vs 35; laminated limestone samples from west  
1580 Somerset coast alone, 7. The average %TOC<sub>cf</sub> values and their uncertainties in the different  
1581 rock types are consistent with the limestones formed by carbonate cementation of light marls  
1582 and with the laminated limestones formed by carbonate cementation of laminated shales.

1583

1584 Figure 2.

1585 (a) Scatter plots of field measurements of vol MS, and laboratory measurements of wt MS and  
1586 %CaCO<sub>3</sub>. The dashed lines indicate the 95% confidence intervals of the regressions.  $N$  =  
1587 number of samples,  $r$  = Pearson's  $r$  (degree of correlation).  $\circ$  = sample from Lyme Regis,  $+$  =  
1588 sample from West Somerset coast. The stratigraphic locations of the samples are indicated in  
1589 Figs 4 and 5.

1590 (b) Profiles of vol MS and %CaCO<sub>3</sub> measurements at Lyme Regis in beds 13 to 23 (bed  
1591 numbers from Lang, 1924).  $+$  = measurement of vol MS, wt MS or %CaCO<sub>3</sub>,  $\circ$  = estimated  
1592 %CaCO<sub>3</sub> based on regression between vol MS and %CaCO<sub>3</sub> (Fig. 2a) – see text Section 3.b.

1593 (c) Profiles of measurements of  $\delta^{18}\text{O}$  and  $\delta^{13}\text{C}$  and %TOC at Lyme Regis in beds 13 to 23.  $+$  =  
1594 bulk sample  $\delta^{18}\text{O}$  and  $\delta^{13}\text{C}$  from Weedon (1987a),  $\square$  = bulk sample  $\delta^{18}\text{O}$  and  $\delta^{13}\text{C}$  from Paul,  
1595 Allison, & Brett (2008),  $\circ$  = *Gryphaea* sp. sample  $\delta^{18}\text{O}$  and  $\delta^{13}\text{C}$  from Weedon (1987a). Key  
1596 to rock-types in Fig. 3.

1597

1598 Figure 3. Lithostratigraphic log, vol MS measurements and ammonite biostratigraphy at St.  
1599 Mary's Well Bay, Lavernock, Wales. Homogeneous limestone nodules are indicated by black  
1600 ellipses. Laminated limestone nodules are indicated by white ellipses. At the levels where vol  
1601 MS was measured within limestone nodules rather than light marl, the nodules are indicated  
1602 on the right of the lithostratigraphic log. Bed numbers from Waters & Lawrence (1987).

1603

1604 Figure 4. Lithostratigraphic log, vol MS and %CaCO<sub>3</sub> measurements and ammonite  
1605 biostratigraphy to the west of Lyme Regis, Devon. The location of the base of the Angulata  
1606 Zone is discussed in Section 5.a. For key to lithologies see Fig. 3. The concentration of samples  
1607 at the level of bed 37 relates to the profile shown in Figs 2b and 2c. ○ = sample measured for  
1608 %CaCO<sub>3</sub> plotted with reference to lower horizontal axis, B = level with abundant calcite beef,  
1609 Lport Mbr = Langport Member, Angul. = Angulata, Buc. = Bucklandi, Extra. = Extranodosa,  
1610 Ext. = Extranodosa. Bed numbers from Lang (1924). Lang (1924) and Hesselbo & Jenkyns  
1611 (1995) provide the names of limestone beds on the Devon/Dorset coast.

1612

1613 Figure 5. (a) Lithostratigraphic log, vol MS and %CaCO<sub>3</sub> measurements and ammonite  
1614 biostratigraphy at St Audries Bay, Somerset. For key to lithologies see Fig. 3. Black circles  
1615 indicate samples measured for %CaCO<sub>3</sub> plotted with reference to lower horizontal axis. ○ =  
1616 sample measured for %CaCO<sub>3</sub> plotted with reference to lower horizontal axis, B = level with  
1617 abundant calcite beef. Bed numbering from Whittaker and Green (1983). (b) As for 5a but a  
1618 composite section from St Audries Bay and Quantock's Head. The join (splice) of the St  
1619 Audries Bay section (St A.) with the Quantocks Head section (Q. H.) is indicated within bed  
1620 96 (Section 3.a). GSSP = Global Stratigraphic Section and Point.

1621

1622 Figure 6. Lithostratigraphic log, vol MS measurements and ammonite biostratigraphy at  
1623 Southam Quarry, near Southam and Long Itchington, Warwickshire. For key to lithologies see  
1624 Fig. 3. L. M. = Langport Member. Bed numbers from Clements *et al.* (1975).

1625

1626 Figure 7.

1627 (a) Photomicrograph of dark marl thin-section (plane polarized light, width of view 3 mm).  
1628 Sample BL120 and Fig. 2.2M of Weedon, (1987a) bed 32a, Rotiforme Subzone, Bucklandi  
1629 Zone, Lyme Regis.

1630 (b) SEM photograph showing coccoliths *in situ* partly engulfed by euhedral microspar  
1631 overgrowth (width of view 14  $\mu\text{m}$ ). Dark marl sample BL120 and Fig. 2.4G of Weedon  
1632 (1987a), bed 32a, Bucklandi Zone, Lyme Regis.

1633 (c) SEM photograph showing an aggregate of coccoliths surrounded by a matrix of organic  
1634 matter and clay (width of view 56  $\mu\text{m}$ ). Dark marl sample BL120 and Fig. 2.4F of Weedon  
1635 (1987a), bed 32a, Bucklandi Zone, Lyme Regis.

1636 (d) SEM photograph showing an aggregate of coccoliths next to *Schizosphaerella punctulata*  
1637 (centre) both surrounded by a matrix of organic matter, clay and calcite microspar (width of  
1638 view 53  $\mu\text{m}$ ). Laminated shale sample BL117, and Fig. 2.4H of Weedon (1987a), topmost  
1639 laminated shale of bed 32, Bucklandi Zone, Lyme Regis.

1640 (e) SEM photograph showing a corroded coccolith in limestone (width of view  $\sim 8 \mu\text{m}$ ).  
1641 Limestone sample BL103 and Fig. 2.4A of Weedon (1987a), bed 29, Conybeari Subzone,  
1642 Bucklandi Zone, Lyme Regis.

1643

1644 Figure 8. Shaw plot constructed using the joint locations of biohorizon bases and biohorizon  
1645 tops at Lyme Regis and the West Somerset Coast (St Audries Bay and Quantock's Head  
1646 sections) as listed in Table 1. The location of the base of the Angulata Zone at Lyme Regis has  
1647 been estimated using the West Somerset data via the line of correlation data (long grey arrows,  
1648 Section 5.a). The ratios of the thicknesses of subzones in the West Somerset composite section  
1649 to subzones in the Lyme Regis section are indicated at the bottom of the plot. Vertical or  
1650 horizontal arrows with bed numbers indicate the levels at which breaks in slope of the line of  
1651 correlation imply relative condensation or intra-formational hiatuses. + = St Audries Bay

1652 section versus Lyme Regis section, × Quantock's Head section versus Lyme Regis section.

1653 Tilm. = Tilmanni, Planorb. = Planorbis, Pl. = Planorbis, Jo. = Johnsoni, Laq. = Laqueus, Extran.

1654 = Extranodosa, Depr. = Depressa, Conyb. = Conybeari, Roti. = Rotiforme.

1655

1656 Figure 9.

1657 (a) Photograph of polished limestone section showing bored and encrusted limestone intraclast

1658 with a hardground-like surface (diagrammatic description below) collected *in situ* from within

1659 bed 25 (Top Copper) below Devonshire Head, Lyme Regis. *i*) Photographic negative image of

1660 acetate peel showing *Liostrea* encrusting the intraclast surface and overlain by bioclastic

1661 packstone. Two *Liostrea* individuals (left and right) encrust a third individual – demonstrating

1662 at least two generations of encrustation. Short arrows indicate the *Talpina ramosa* Von

1663 Hagenow borings into the intraclast surface and within the encrusting *Liostrea*. *ii*) As for *i*) but

1664 a different section of the intraclast surface (see diagram for location).

1665 (b) Limestone intraclasts on the surface of a fallen block of limestone, Monmouth Beach, Lyme

1666 Regis. The lens cap is 5 cm in diameter.

1667 (c) Protrusive *Diplocraterion* forming dark marl burrow-fill within limestone bed 19

1668 (Specketty), Seven Rock Point, Lyme Regis.

1669 (d) Horizon of isolated dark marl burrow fills indicating the former presence of a bed of dark

1670 marl that has been removed locally by seafloor erosion, bed 19, Seven Rock Point, Lyme Regis.

1671

1672 Figure 10.

1673 (a) Compilation of oxygen- and carbon-isotope measurements for Lyme Regis from the

1674 Angulata and Bucklandi Zones. Note several data points from limestone beds (black squares)

1675 near  $\delta^{18}\text{O} = -4.5$  and  $\delta^{13}\text{C} = -1.5$  ‰ VPDB are obscured by the data for marl or laminated shale

1676 (unfilled triangles). Sources of measurements for whole-rock: Campos and Hallam (1979);

1677 Gluyas (1984); Weedon (1987a); Arzani (2004; 2006); Paul, Allison & Brett (2008), for  
1678 *Gryphaea* sp.: Weedon (1987a).

1679 (b) Compilation of oxygen- and carbon-isotope measurements for West Somerset Coast (Kilve)  
1680 for the Bucklandi Zone. Sources of measurements for whole rock: Allison, Hesselbo & Brett  
1681 (2008); Price, Vowles-Sheridan & Anderson (2008). Measurements plotted exclude atypical  
1682 rock-types associated with the Bucklandi Zone mud mounds.

1683 (c) Compilation of oxygen- and carbon-isotope measurements for West Somerset Coast (St  
1684 Audries and Doniford) for the Tilmanni and Planorbis Zones. Sources of measurements for  
1685 whole rock: Arzani (2004; 2006); Clémence *et al.* (2010 as listed in Supplementary information  
1686 of Paris *et al.*, 2010); for *Liostrea* sp.: van Schootbrugge *et al.*, (2007, their ‘unaltered’ samples  
1687 only).

1688 Table 1. Ammonite biohorizon limits on the West Somerset (St Audries Bay and Quantock's  
 1689 Head), Devon/Dorset (Lyme Regis) and South Wales (Lavernock) coast sections.

1690

---

1691

Zone	Subzone	Biohorizon	Pos.	St A.	Qu. H.	CWS	Lav.	L.R.
Bucklandi	Rotiforme	Sn7 <i>rotiforme</i>	Base	-	92.69	92.69	-	18.06
Bucklandi	Rotiforme	Sn6 cf. <i>defneri</i>	Top	-	90.66	90.66	-	17.94
Bucklandi	Rotiforme	Sn6 cf. <i>defneri</i>	Base	-	90.38	90.38	-	17.90
Bucklandi	Rotiforme	Sn5c <i>silvestri</i>	Top	-	87.76	87.76	-	17.76
Bucklandi	Rotiforme	Sn5c <i>silvestri</i>	Base	-	87.70	87.70	-	17.70
Bucklandi	Conybeari	Sn5b <i>conybeari</i>	Top	-	86.72	86.72	-	17.56
Bucklandi	Conybeari	Sn5b <i>conybeari</i>	Base	-	86.52	86.52	-	17.43
Bucklandi	Conybeari	Sn5a <i>elegans</i>	Top	-	86.48	86.48	-	-
Bucklandi	Conybeari	Sn5a <i>elegans</i>	Base	-	86.16	86.16	-	-
Bucklandi	Conybeari	Sn4 <i>rotator</i>	Top	-	82.40	82.40	-	16.78
Bucklandi	Conybeari	Sn4 <i>rotator</i>	Base	-	82.32	82.32	-	16.76
Bucklandi	Conybeari	Sn3b <i>rouvillei</i>	Top	-	81.64	81.64	-	16.64
Bucklandi	Conybeari	Sn3b <i>rouvillei</i>	Base	-	81.46	81.46	-	16.40
Bucklandi	Conybeari	Sn3a <i>rotarius</i>	Top	-	81.28	81.28	-	16.14
Bucklandi	Conybeari	Sn3a <i>rotarius</i>	Base	-	81.18	81.18	-	16.12
Bucklandi	Conybeari	Sn2b <i>conybearoides</i>	Top	-	79.98	79.98	-	-
Bucklandi	Conybeari	Sn2b <i>conybearoides</i>	Base	-	79.78	79.78	-	-
Bucklandi	Conybeari	Sn2a <i>Metophioceras</i> sp. A	Top	-	79.34	79.34	-	-
Bucklandi	Conybeari	Sn2a <i>Metophioceras</i> sp. A	Base	-	78.64	78.64	-	15.22
Bucklandi	Conybeari	Sn1 <i>quantoxense</i>	Top	-	78.14	78.14	-	15.21
Bucklandi	Conybeari	Sn1 <i>quantoxense</i>	Base	-	78.06	78.06	-	15.16
Angulata	Depressa	Hn27b <i>quadrata</i> 2	Top	-	77.50	77.50	-	14.96
Angulata	Depressa	Hn27b <i>quadrata</i> 2	Base	-	77.42	77.42	-	14.94
Angulata	Depressa	Hn27a <i>quadrata</i> 1	Top	-	73.42	73.42	-	-
Angulata	Depressa	Hn27a <i>quadrata</i> 1	Base	-	73.38	73.38	-	14.56
Angulata	Depressa	Hn26b <i>princeps</i>	Top	-	72.14	72.14	-	13.66
Angulata	Depressa	Hn26b <i>princeps</i>	Base	-	72.04	72.04	-	13.50
Angulata	Depressa	Hn26a <i>depressa</i> 1	Top	-	69.94	69.94	-	-
Angulata	Depressa	Hn26a <i>depressa</i> 1	Base	-	69.52	69.52	-	13.36
Angulata	Complanata	Hn25 <i>striatissima</i>	Top	-	67.10	67.10	-	-
Angulata	Complanata	Hn25 <i>striatissima</i>	Base	-	66.90	66.90	-	-
Angulata	Complanata	Hn24d grp. <i>vaihingensis</i>	Top	-	65.68	65.68	-	-
Angulata	Complanata	Hn24d grp. <i>vaihingensis</i>	Base	-	65.26	65.26	-	-
Angulata	Complanata	Hn24c aff. <i>complanata</i>	Top	-	63.78	63.78	-	12.58
Angulata	Complanata	Hn24c aff. <i>complanata</i>	Base	-	63.60	63.60	-	12.46
Angulata	Complanata	Hn24b <i>phoebetica</i>	Top	-	63.14	63.14	-	-
Angulata	Complanata	Hn24b <i>phoebetica</i>	Base	-	63.04	63.04	-	-
Angulata	Complanata	Hn24a <i>complanata</i>	Top	-	57.40	57.40	-	12.22
Angulata	Complanata	Hn24a <i>complanata</i>	Base	-	57.26	57.26	-	12.12
Angulata	Complanata	Hn23c cf. <i>polyeides</i>	Top	54.74	-	54.74	-	-
Angulata	Complanata	Hn23c cf. <i>polyeides</i>	Base	54.60	-	54.60	-	-
Angulata	Complanata	Hn23b <i>similis</i>	Top	52.66	52.09	52.66	-	12.10
Angulata	Complanata	Hn23b <i>similis</i>	Base	52.58	51.95	52.58	-	12.06
Angulata	Complanata	Hn23a grp. <i>stenorhyncha</i>	Top	49.48	-	49.48	-	12.00
Angulata	Complanata	Hn23a grp. <i>stenorhyncha</i>	Base	49.26	-	49.26	-	11.90
Angulata	Extranodosa	Hn22 cf. <i>germanica</i>	Top	47.42	51.24	47.42	-	-
Angulata	Extranodosa	Hn22 cf. <i>germanica</i>	Base	47.22	51.02	47.22	-	-
Angulata	Extranodosa	Hn21c <i>amblygonia</i> 3	Top	45.40	-	45.40	-	11.36
Angulata	Extranodosa	Hn21c <i>amblygonia</i> 3	Base	45.00	-	45.00	-	11.28
Angulata	Extranodosa	Hn21b cf. <i>pyncotycha</i>	Top	43.26	-	43.26	-	-
Angulata	Extranodosa	Hn21b cf. <i>pyncotycha</i>	Base	43.12	-	43.12	-	-
Angulata	Extranodosa	Hn21a <i>atrox</i>	Top	42.24	-	42.24	-	-

Angulata	Extranodosa	Hn21a <i>atrox</i>	Base	42.14	-	42.14	-	-
Angulata	Extranodosa	Hn20c <i>hadrotychus</i>	Top	40.86	-	40.86	-	-
Angulata	Extranodosa	Hn20c <i>hadrotychus</i>	Base	40.76	-	40.76	-	-
Angulata	Extranodosa	Hn20b <i>Schlotheimia</i> sp. 1b	Top	40.64	-	40.64	-	-
Angulata	Extranodosa	Hn20b <i>Schlotheimia</i> sp. 1b	Base	40.58	-	40.58	-	-
Angulata	Extranodosa	Hn20a <i>Schlotheimia</i> sp. 1a	Top	40.08	-	40.08	-	-
Angulata	Extranodosa	Hn20a <i>Schlotheimia</i> sp. 1a	Base	39.96	40.10	39.96	-	<b>10.54</b>
Liasicus	Laqueus	Hn19d aff. <i>bloomfieldense</i>	Top	39.72	-	39.72	-	-
Liasicus	Laqueus	Hn19d aff. <i>bloomfieldense</i>	Base	39.60	-	39.60	-	-
Liasicus	Laqueus	Hn19c <i>bloomfieldense</i>	Top	38.80	-	38.80	-	-
Liasicus	Laqueus	Hn19c <i>bloomfieldense</i>	Base	38.66	-	38.66	-	-
Liasicus	Laqueus	Hn19b cf. <i>subliassicus</i>	Top	37.22	-	37.22	-	-
Liasicus	Laqueus	Hn19b cf. <i>subliassicus</i>	Base	36.98	-	36.98	-	-
Liasicus	Laqueus	Hn19a cf. <i>laqueolus</i>	Top	36.80	-	36.80	-	-
Liasicus	Laqueus	Hn19a cf. <i>laqueolus</i>	Base	36.32	-	36.32	-	-
Liasicus	Laqueus	Hn18d cf. <i>polyspeirum</i>	Top	35.80	-	35.80	-	-
Liasicus	Laqueus	Hn18d cf. <i>polyspeirum</i>	Base	35.68	-	35.68	-	-
Liasicus	Laqueus	Hn18c cf. <i>costatum</i>	Top	33.96	-	33.96	-	9.66
Liasicus	Laqueus	Hn18c cf. <i>costatum</i>	Base	33.46	-	33.46	-	9.53
Liasicus	Laqueus	Hn18b cf. <i>gallbergensis</i>	Top	33.08	34.74	33.08	-	9.25
Liasicus	Laqueus	Hn18b cf. <i>gallbergensis</i>	Base	33.00	34.21	33.00	-	9.18
Liasicus	Laqueus	Hn 18a <i>laqueus</i>	Top	33.00	33.81	33.00	-	9.03
Liasicus	Laqueus	Hn 18a <i>laqueus</i>	Base	32.88	33.53	32.88	-	8.97
Liasicus	Portlocki	Hn17c cf. <i>latimontanum</i>	Top	32.48	33.10	32.48	-	8.94
Liasicus	Portlocki	Hn17c cf. <i>latimontanum</i>	Base	32.28	32.92	32.28	-	-
Liasicus	Portlocki	Hn17b aff. <i>beneckeii</i>	Top	29.94	-	29.94	-	-
Liasicus	Portlocki	Hn17b aff. <i>beneckeii</i>	Base	29.86	-	29.86	-	-
Liasicus	Portlocki	Hn17a cf. <i>gottिंगense</i>	Top	29.14	-	29.14	-	-
Liasicus	Portlocki	Hn17a cf. <i>gottिंगense</i>	Base	28.94	-	28.94	-	8.84
Liasicus	Portlocki	Hn16b grp. <i>portlocki</i>	Top	28.46	-	28.46	-	8.80
Liasicus	Portlocki	Hn16b grp. <i>portlocki</i>	Base	28.16	-	28.16	-	8.70
Liasicus	Portlocki	Hn16a cf. <i>crassicosta</i>	Top	27.20	-	27.20	-	-
Liasicus	Portlocki	Hn16a cf. <i>crassicosta</i>	Base	25.92	-	25.92	-	-
Liasicus	Portlocki	Hn15 <i>hagenowi</i>	Top	25.62	-	25.62	-	8.21
Liasicus	Portlocki	Hn15 <i>hagenowi</i>	Base	25.12	-	25.12	-	8.16
Liasicus	Portlocki	Hn14d <i>harpotychum</i>	Top	19.16	-	19.16	-	-
Liasicus	Portlocki	Hn14d <i>harpotychum</i>	Base	19.11	-	19.11	-	-
Liasicus	Portlocki	Hn14c <i>Waehneroceras</i> sp. nov.	Top	17.68	-	17.68	-	-
Liasicus	Portlocki	Hn14c <i>Waehneroceras</i> sp. nov.	Base	17.44	-	17.44	-	-
Liasicus	Portlocki	Hn14b <i>iapetus</i>	Top	15.60	-	15.60	-	6.66
Liasicus	Portlocki	Hn14b <i>iapetus</i>	Base	13.92	-	13.92	-	6.61
Liasicus	Portlocki	Hn14a aff. <i>franconium</i>	Top	13.62	-	13.62	14.67	-
Liasicus	Portlocki	Hn14a aff. <i>franconium</i>	Base	13.54	-	13.54	14.58	6.58
Planorbis	Johnstoni	Hn13c 'post'- <i>intermedium</i>	Top	13.50	-	13.50	14.46	-
Planorbis	Johnstoni	Hn13c 'post'- <i>intermedium</i>	Base	13.42	-	13.42	14.19	-
Planorbis	Johnstoni	Hn13b grp. <i>intermedium</i>	Top	13.10	-	13.10	12.93	6.42
Planorbis	Johnstoni	Hn13b grp. <i>intermedium</i>	Base	12.82	-	12.82	12.84	-
Planorbis	Johnstoni	Hn13a aff. <i>torus</i>	Top	-	-	-	12.51	-
Planorbis	Johnstoni	Hn13a aff. <i>torus</i>	Base	-	-	-	12.39	6.08
Planorbis	Johnstoni	Hn12 <i>johnstoni</i>	Top	12.48	-	12.48	12.12	5.90
Planorbis	Johnstoni	Hn12 <i>johnstoni</i>	Base	12.10	-	12.10	11.43	5.86
Planorbis	Johnstoni	Hn11d <i>Caloceras</i> sp. 5	Top	-	-	-	10.77	-
Planorbis	Johnstoni	Hn11d <i>Caloceras</i> sp. 5	Base	-	-	-	10.65	-
Planorbis	Johnstoni	Hn11c <i>Caloceras</i> sp. 4	Top	11.30	-	11.30	10.53	-
Planorbis	Johnstoni	Hn11c <i>Caloceras</i> sp. 4	Base	11.22	-	11.22	10.41	-
Planorbis	Johnstoni	Hn11b aff. <i>tortlie</i>	Top	10.94	-	10.94	10.17	5.20
Planorbis	Johnstoni	Hn11b aff. <i>tortlie</i>	Base	10.78	-	10.78	10.11	5.14
Planorbis	Johnstoni	Hn11a <i>Caloceras</i> sp. 2	Top	10.02	-	10.02	-	-
Planorbis	Johnstoni	Hn11a <i>Caloceras</i> sp. 2	Base	9.98	-	9.98	-	5.06
Planorbis	Johnstoni	Hn10 aff. <i>aries</i>	Top	9.82	-	9.82	9.87	-



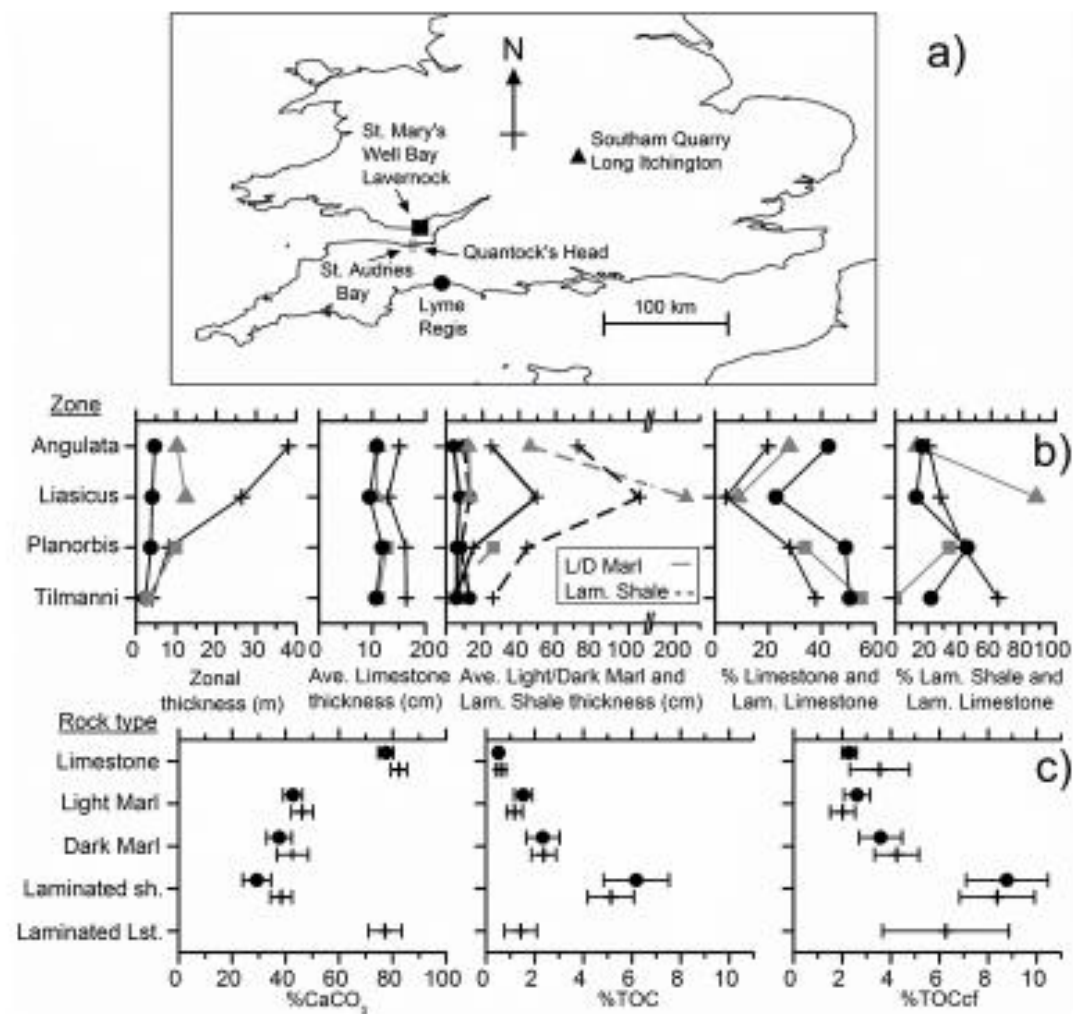
Planorbis	Johnstoni	Hn10 aff. <i>aries</i>	Base	9.66	-	9.66	9.72	4.88
Planorbis	Planorbis	Hn9 <i>bristoviense</i>	Top	-	-	-	9.45	4.79
Planorbis	Planorbis	Hn9 <i>bristoviense</i>	Base	-	-	-	9.39	4.76
Planorbis	Planorbis	Hn8 <i>sampsoni</i>	Top	-	-	-	8.25	-
Planorbis	Planorbis	Hn8 <i>sampsoni</i>	Base	-	-	-	8.10	-
Planorbis	Planorbis	Hn7 <i>plicatulum</i>	Top	9.08	-	9.08	7.44	3.78
Planorbis	Planorbis	Hn7 <i>plicatulum</i>	Base	8.78	-	8.78	7.35	3.72
Planorbis	Planorbis	Hn6 <i>planorbis</i> $\beta$	Top	8.58	-	8.58	6.93	3.70
Planorbis	Planorbis	Hn6 <i>planorbis</i> $\beta$	Base	8.18	-	8.18	6.72	3.66
Planorbis	Planorbis	Hn5 <i>planorbis</i> $\alpha$	Top	8.18	-	8.18	6.72	3.66
Planorbis	Planorbis	Hn5 <i>planorbis</i> $\alpha$	Base	5.98	-	5.98	6.33	3.42
Planorbis	Planorbis	Hn4 <i>antecedens</i>	Top	5.58	-	5.58	6.15	3.02
Planorbis	Planorbis	Hn4 <i>antecedens</i>	Base	5.42	-	5.42	6.06	2.94
Planorbis	Planorbis	Hn3 <i>imitans</i>	Top	-	-	-	5.49	-
Planorbis	Planorbis	Hn3 <i>imitans</i>	Base	5.42	-	5.42	4.71	2.82
Tilmanni		Hn2 <i>erugatum</i>	Top	5.38	-	5.38	4.65	-
Tilmanni		Hn2 <i>erugatum</i>	Base	5.26	-	5.26	4.56	-
Tilmanni		Hn1 (no ammonites)	Top	5.26	-	5.26	4.56	-
Tilmanni		Hn1 (no ammonites)	Base	?1.50	-	?1.50	?1.86	?0.60

1692

1693 Height in metres of biohorizon boundaries above base of the Blue Lias Formation. The value  
1694 in ***bold italics*** for the base Angulata Zone at Lyme Regis was estimated using the correlation  
1695 with the St. Audries Bay section (see Fig. 8, Section 5.a.). Pos. = Position, St A. = St Audries  
1696 Bay section, Somerset, Qu. H. = Quantock's Head section, Somerset, CWS = Composite West  
1697 Somerset coastal sections using common splice level at 56.90 m (below this level the heights  
1698 for Quantock's Head differ from the CWS heights), Lav. = St. Mary's Well Bay section near  
1699 Lavernock, South Wales, L.R. = Pinhay Bay to Devonshire Head section, Lyme Regis, Dorset.

1700

Fig. 1



1701

1702

1703



Fig. 3

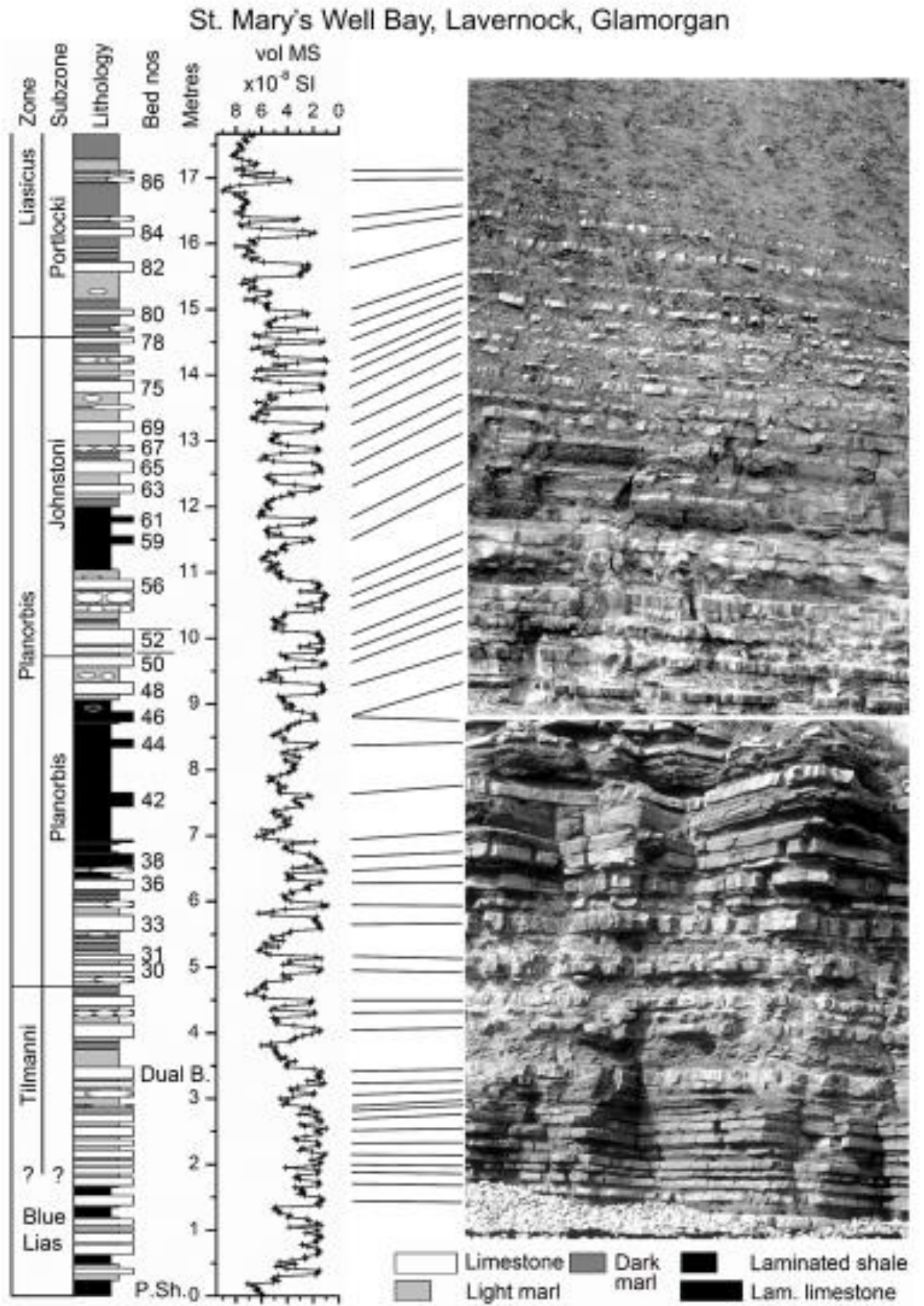


Fig. 4

Lyme Regis (Pinhay Bay – Devonshire Head), Devon

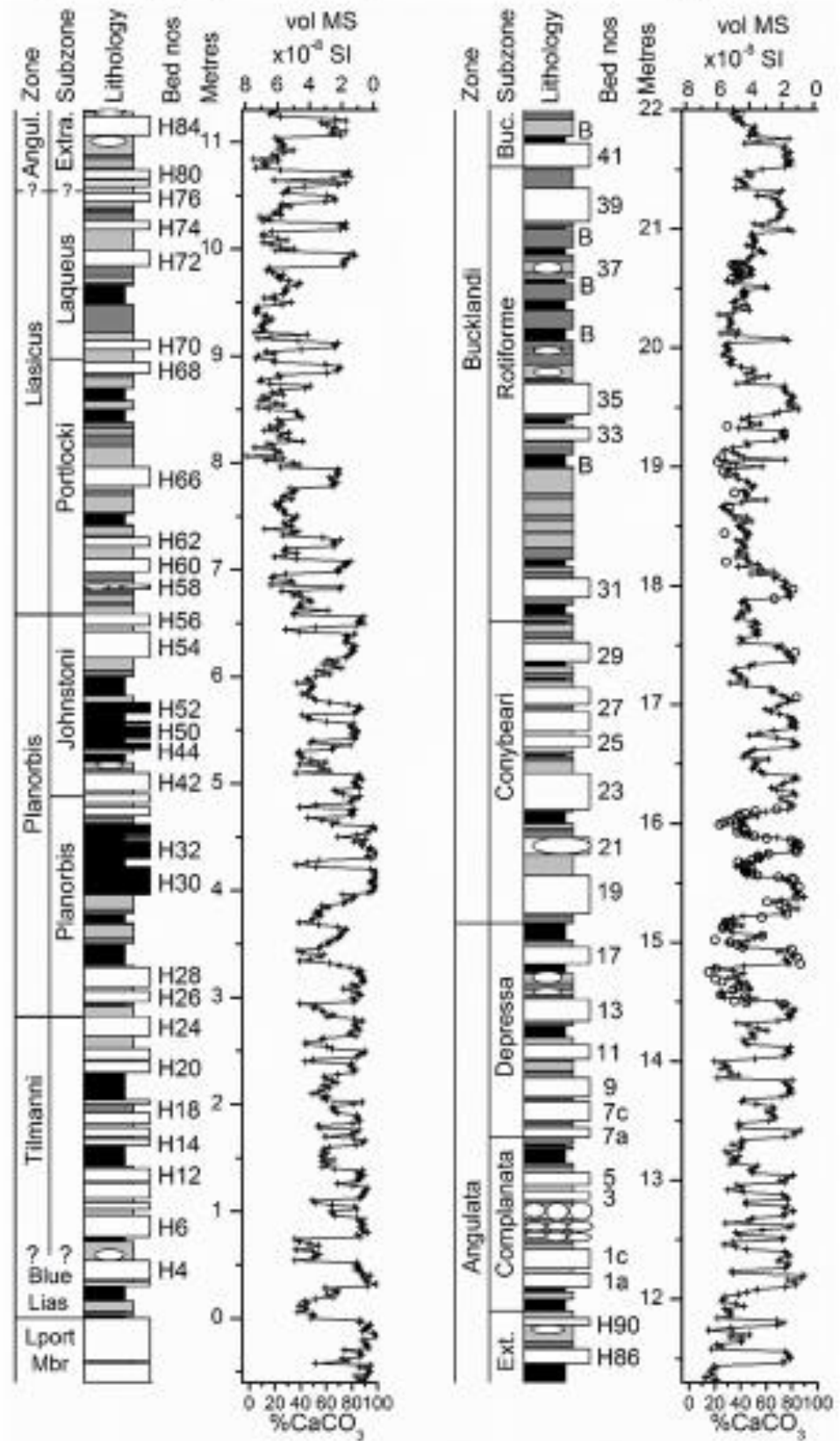




Fig. 5a

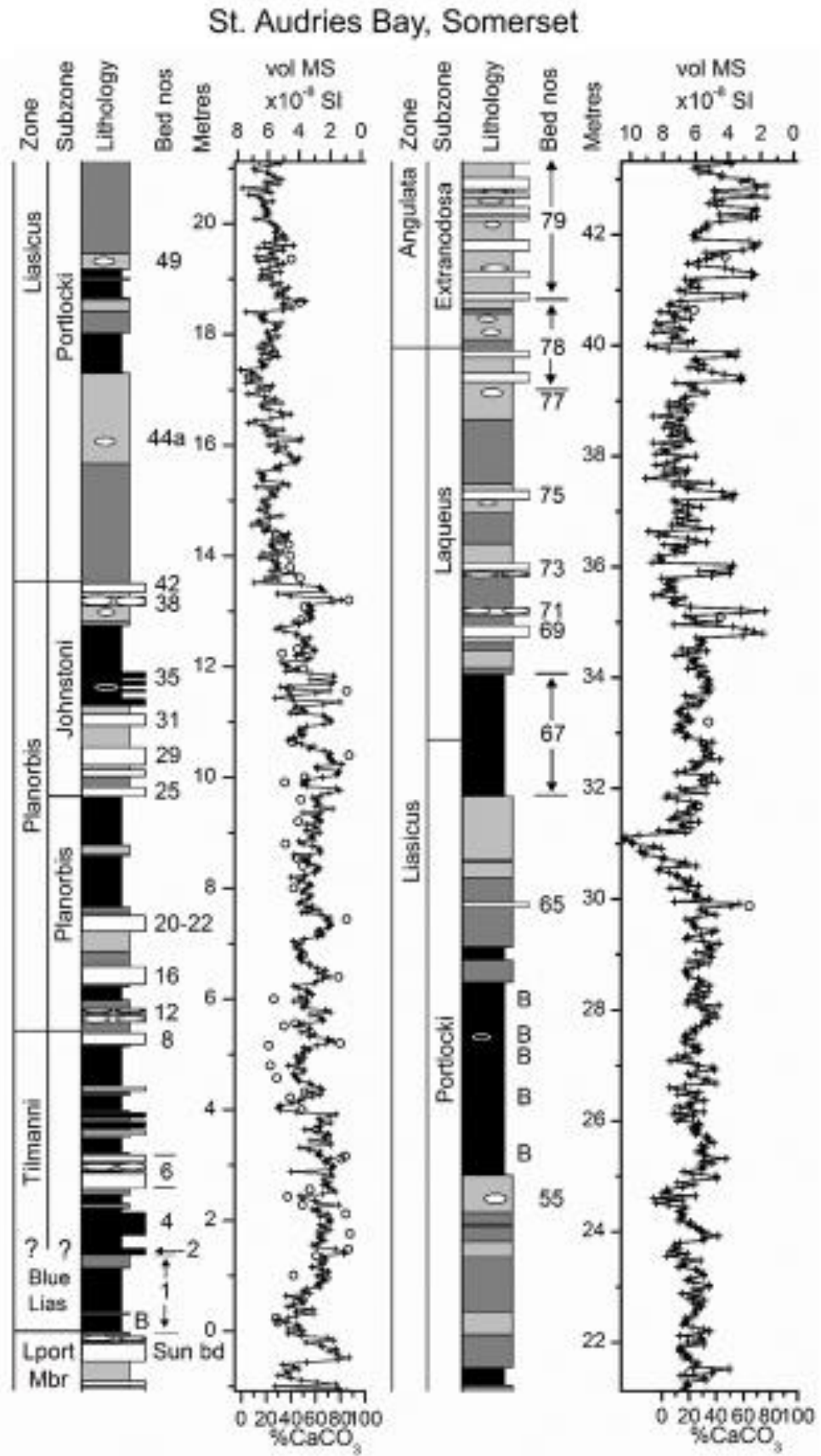


Fig. 5b

St. Audries Bay – Quantock's Head, Somerset

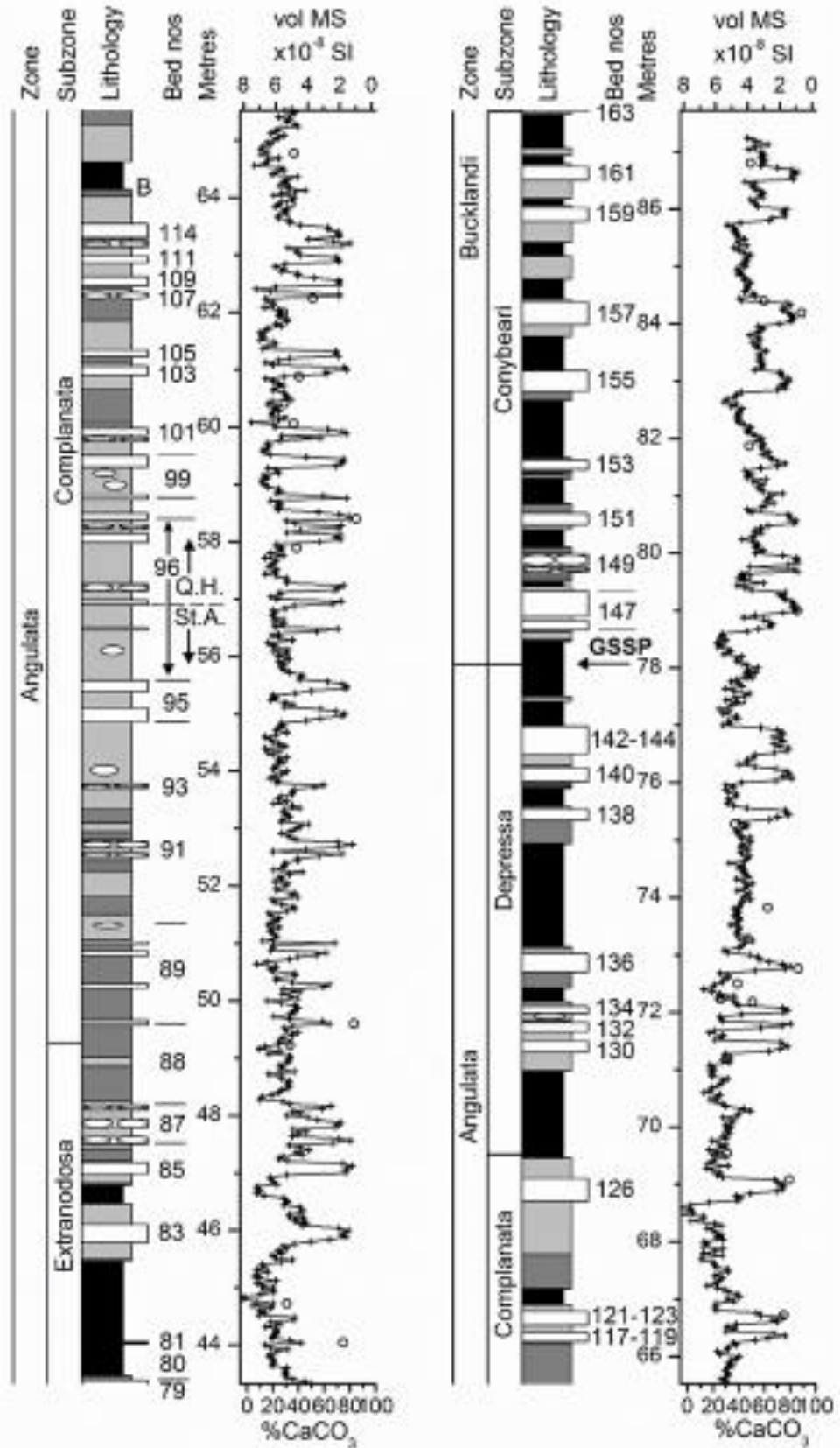


Fig. 6

Southam Quarry, Long Itchington, Warwickshire

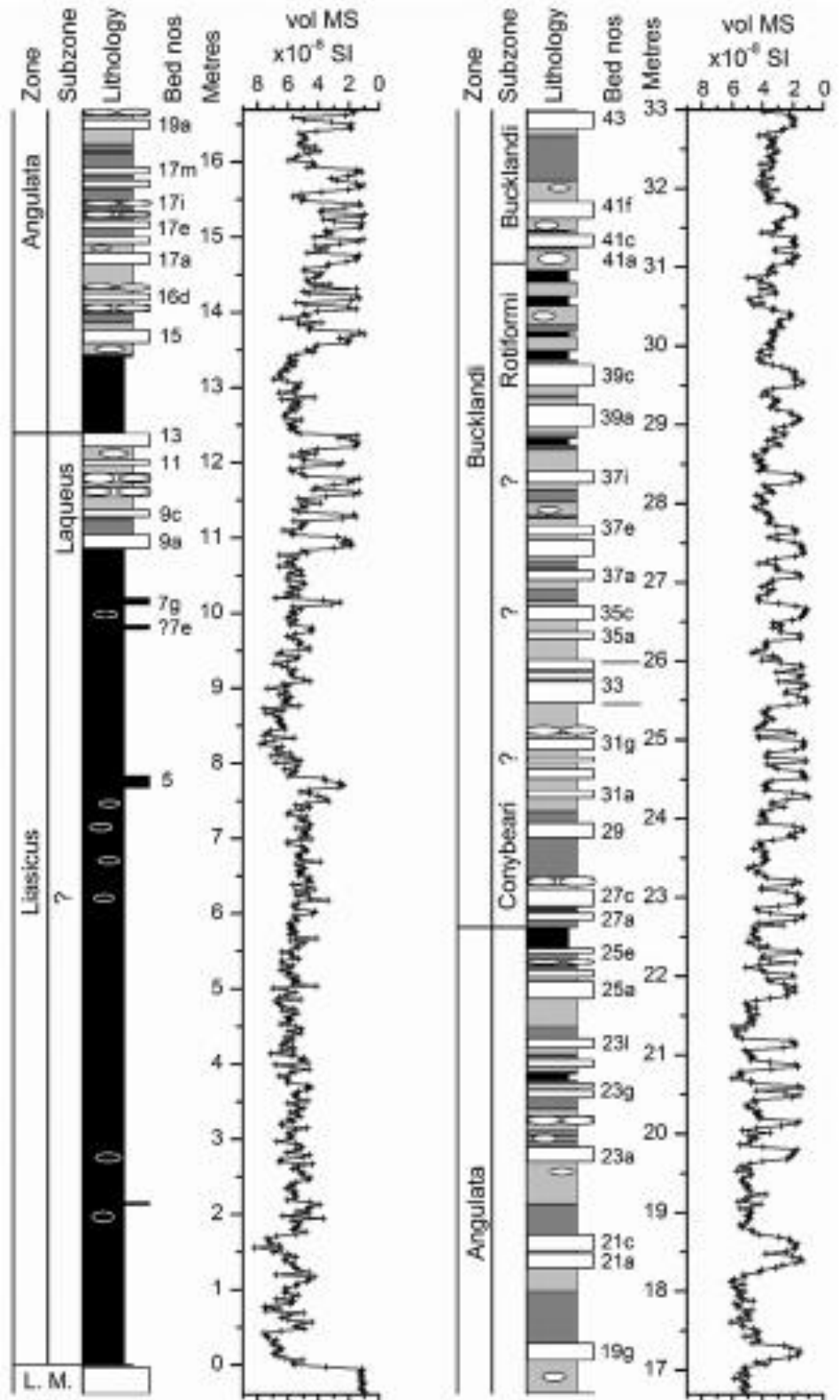
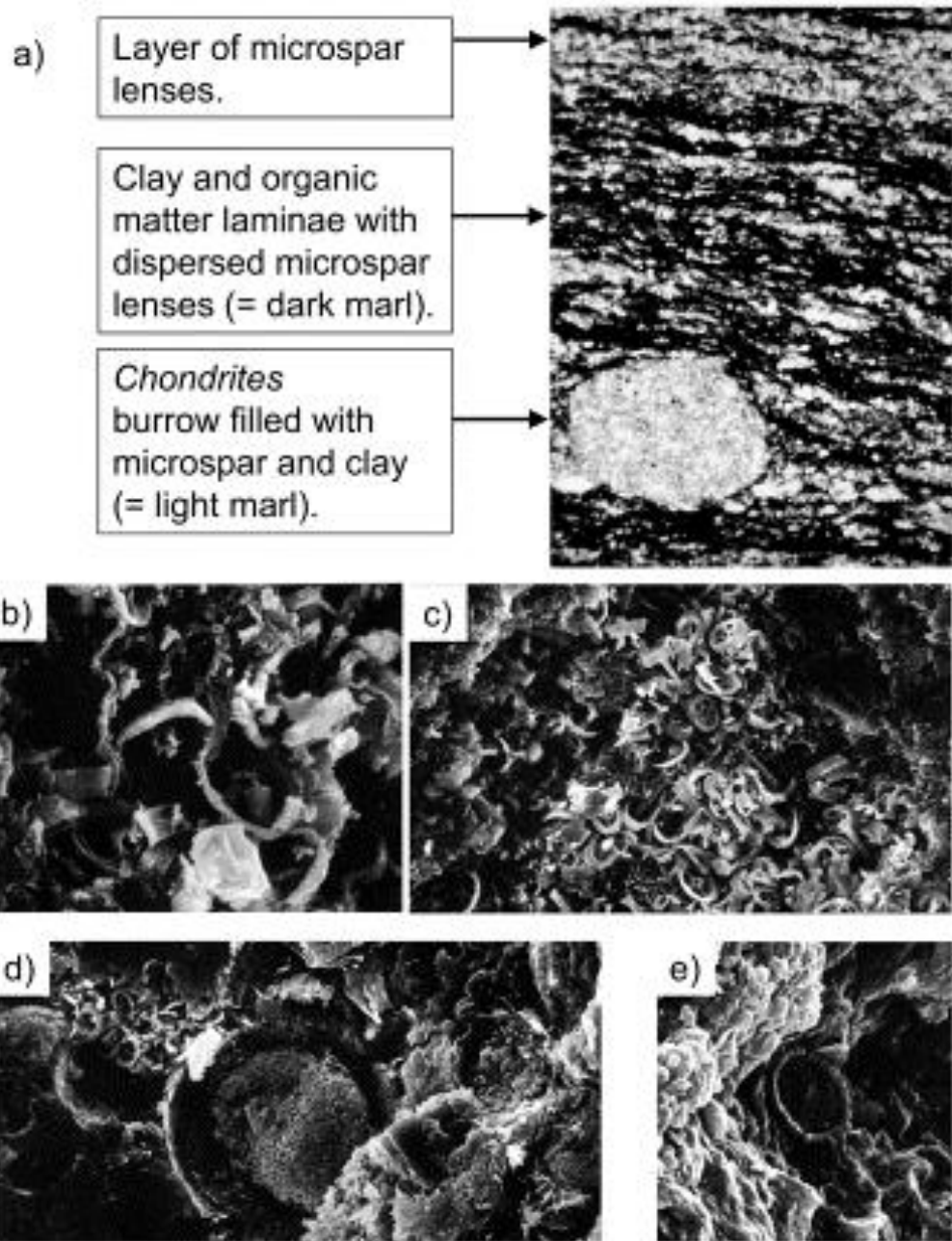




Fig. 7



1712

1713

Fig. 8

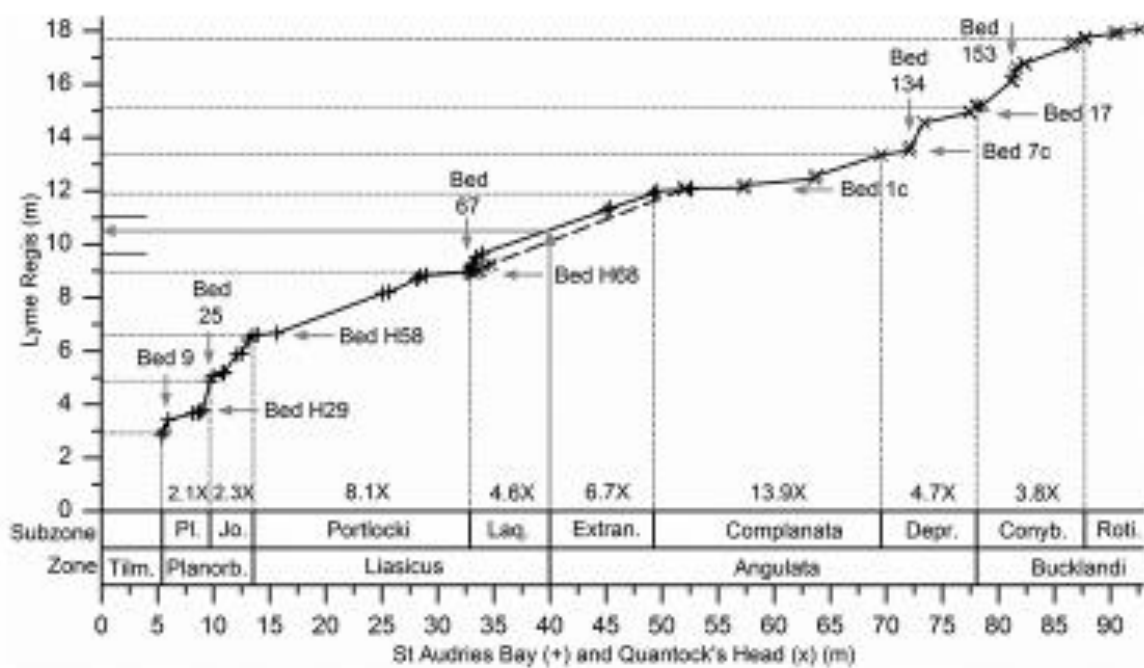


Fig. 9

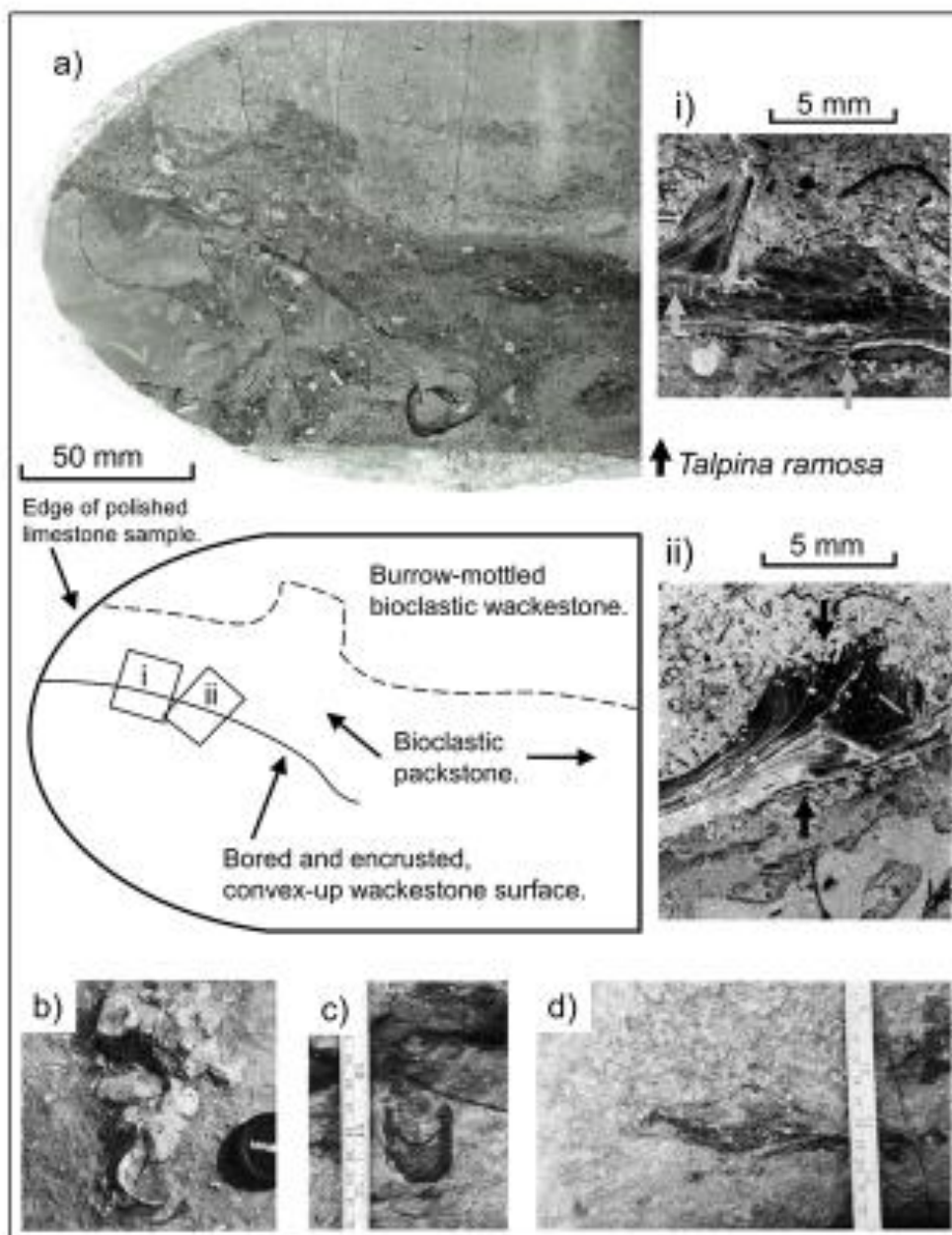


Fig. 10

